

1        **Improved model for human induced vibrations of high-frequency floors**

2        **A. S. Mohammed<sup>1</sup>, A. Pavic<sup>1</sup>, V. Racic<sup>2</sup>**

3        <sup>1</sup> Vibration Engineering Section, College of Engineering, Mathematics and Physical Sciences,  
4        University of Exeter, North Park Road, EX4 4QF, Exeter, UK

5        <sup>2</sup> Department of Civil and Environmental Engineering, Politecnico di Milano, Piazza  
6        Leonardo da Vinci 32, 20133 Milan, Italy

7        Contact author:        Ahmed S. Mohammed  
8                                College of Engineering, Mathematics and Physical Sciences  
9                                University of Exeter  
10                              North Park Road  
11                              Exeter EX4 4QF  
12                              E-mail: asm221@exeter.ac.uk  
13                              Tel: 0114-2225721  
14

15        Body text word count: 6900

16        Number of figures: 23

17        Number of tables: 1

18

19 **Abstract**

20 The key UK design guidelines published by the Concrete Society and Concrete Centre for single human  
21 walking excitation of high-frequency floors were introduced more than 10 years ago. The corresponding  
22 walking force model is derived using a set of single footfalls recorded on a force plate and it features a  
23 deterministic approach which contradicts the stochastic nature of human-induced loading, including  
24 intra- and inter- subject variability. This paper presents an improved version of this force model for  
25 high-frequency floors with statistically defined parameters derived using a comprehensive database of  
26 walking force time histories, comprising multiple successive footfalls that are continuously measured  
27 on an instrumented treadmill. The improved model enables probability-based prediction of vibration  
28 levels for any probability of non-exceedance, while the existing model allows for vibration prediction  
29 related to 75% probability of non- exceedance for design purposes. Moreover, the improved model  
30 shifts the suggested cut-off frequency between low- and high-frequency floors from 10 Hz to 14 Hz.  
31 This is to account for higher force harmonics that can still induce the resonant vibration response and  
32 to avoid possible significant amplification of the vibration response due to the near-resonance effect.  
33 Minor effects of near-resonance are taken into account by a damping factor. The performance of the  
34 existing and the improved models is compared against numerical simulations carried out using a finite  
35 element model of a structure and the treadmill forces. The results show that while the existing model  
36 tends to overestimate or underestimate the vibration levels depending on the pacing rate, the new model  
37 provides statistically reliable estimations of the vibration responses. Hence, it can be adopted in a new  
38 generation of the design guidelines featuring a probabilistic approach to vibration serviceability  
39 assessment of high-frequency floors.

40 **Keywords:** vibration serviceability, walking excitation, cut-off frequency, probabilistic  
41 modelling.

## 42 **1 Introduction**

43 The advancements in construction materials and design software have boosted the current architectural  
44 trend of building lighter structures than ever with increasingly longer spans and reduced carbon  
45 footprint. While the Ultimate Limit State (ULS) requirements for these modern structures are normally  
46 met, Serviceability Limit State (SLS) criteria increasingly govern design. This is particularly the case  
47 with vibration serviceability of structures due to human activities, such as walking, running and jumping  
48 [1,2].

49 Building floors have traditionally been designed mainly to accommodate people, who are by their nature  
50 very sensitive vibration receivers [3]. Nowadays there is a growing need for floors accommodating  
51 vibration sensitive equipment, such as microscopes and lasers in hospitals and hi-tech laboratories.  
52 Their optimal functioning commonly permits extremely low vibration levels (often micro-levels) of the  
53 supporting structure which are far below human perception. Vibration criteria (VC) for sensitive  
54 equipment is normally provided by the manufacturer, leaving the provision of the adequate floor to  
55 clients and structural designers [2].

56 Early studies made vibration assessment based on static deflection of a floor and suggested increasing  
57 the stiffness and therefore the fundamental frequency to reduce the vibration response. The same  
58 concept features the work by Ungar and White [4] who were the first to use an “idealised footfall force”  
59 [5] in a method to calculate the maximum velocity response. This method has been further developed  
60 by Amick [6] and adopted in a number of design guidelines [7,8].

61 A more sophisticated approach was based on the nature of the vibration response [9,10]. If the response  
62 is dominated by a resonant build-up they are known as *low-frequency floors*, while those that show a  
63 sequence of transient responses due to each successive footfall are called *high-frequency floors*. The  
64 division between low- and high-frequency floors depends on whether the fundamental frequency of the  
65 floor is relatively low or high, respectively. The threshold frequency (known as *cut-off frequency*) varies  
66 significantly for different authors and design guidelines, as shown in **Table 1**.

67 Floors supporting sensitive equipment are required to have low-level transient vibration responses due  
68 to human walking excitation [11,12], thus they should be high-frequency floors. A number of studies  
69 [13,14] reported that the cut-off frequencies given in **Table 1** are too conservative, which has a major  
70 effect on the design and cost of ultra-sensitive facilities. They showed that the resonant build-up  
71 response can occur even for floors with a fundamental frequency of above 15 Hz [14]. This is because  
72 there are higher dominant harmonics of walking loading at frequencies above 10 Hz, which contain a  
73 significant amount of energy. For example, according to the design guidelines, a floor with a  
74 fundamental frequency of 11.5 Hz is a high-frequency floor. However, a person walking at a pacing  
75 rate 2.3 Hz, whose corresponding walking force has Fourier amplitudes shown in **Fig. 1**, still can induce  
76 the resonant vibrations by the harmonic corresponding to the fifth integer multiple of walking loading.  
77 This error in the floor type yields an underestimated vibration response, hence a floor may not be fit for  
78 purpose.

79 The uncertainty linked to the cut-off frequency could be explained by the lack of knowledge and/or  
80 reliable experimental data pertinent to human walking excitation. This study addresses this issue by  
81 determining a cut-off frequency based on detailed numerical analysis featuring a large number of  
82 continuously measured walking forces generated by many people walking on an instrumented treadmill  
83 [15,16]. Another major drawback of the available design guidelines is the deterministic mathematical  
84 description of human-induced loading, while a probabilistic approach is arguably more suitable due to  
85 the inherent stochastic nature of human walking forces [16–19]. This study proposes an improved and  
86 probability-based version of the widely used Arup’s force model for high-frequency floors [20]. This  
87 model was chosen as it provides closest and least conservative predictions of floor vibrations compared  
88 with experimental results [12,14,21,22]. The parameter estimation of the proposed model and the model  
89 implementation take statistical approaches. Moreover, the effect of structural damping is introduced in  
90 this model to take into account any “near-resonance” effects.

91 For high-frequency floors, the time domain modelling approach used here is more appropriate than the  
92 frequency domain approach used elsewhere [17,23,24] due to its capability to describe the peak  
93 responses corresponding to footfall strikes. The performance of the new model has been verified via

94 numerical simulations utilising the treadmill forces and a finite element model of a high-frequency  
95 floor.

96 Section 2 of this paper describes the nature of the human-induced vibration responses and the procedure  
97 followed to derive a more reliable cut-off frequency between low- and high-frequency floors. The new  
98 model and its implementation procedure are elaborated in Section 3, while its verification is  
99 demonstrated in Section 4. Finally, a discussion of the results and the main conclusions are presented  
100 in Section 5.

## 101 **2 Resonant and transient vibration responses due to human walking** 102 **excitation**

103 This section demonstrates the nature of the resonant and transient vibration responses due to human  
104 walking excitation based on numerical simulations using measured walking forces (Section 2.1) applied  
105 to different Single Degree of Freedom (SDOF) oscillators (Section 2.2). Moreover, it aims to derive a  
106 reliable value of the cut-off frequency (Section 2.3) relevant to the model development presented in  
107 Section 4 .

### 108 **2.1 Walking forces**

109 The authors have at their disposal a comprehensive database of 715 continuously measured vertical  
110 force time histories, generated by more than 70 test subjects walking individually on an instrumented  
111 treadmill [15,16]. Each test subject followed the same test protocol designed to record a force signal at  
112 a constant speed of rotation of the treadmill belts per each test. The speed was varied randomly from  
113 slow to fast across successive tests, so the database comprises forces for a wide range of pacing rates.  
114 Each force time history contains at least 60 successive footfalls, rather than a single footfall only used  
115 in development of Arup's model. This makes it possible to study the intra-subject variability of the  
116 walking loads, i.e. the inability of a person to generate two identical footfalls during a walking test. The  
117 large number of test subjects processed in the experiment enables studies of inter-subject variability,  
118 i.e. differences between force records generated by different people under (nominally) identical

119 conditions. These forces can be considered statistically more reliable data than that used in the  
120 development of the original Arup model [25].

121 The range of pacing rates corresponding to these walking forces is between 1.4-2.5 Hz. The force signals  
122 were cropped for the time duration of 50 footfalls from the middle of the force signal. Several first and  
123 last footfalls were discarded to eliminate potential negative effects related to the start and the end of the  
124 walking test, yielding footfalls that might not reliably represent the real walking of a person. This length  
125 of the force signal was used everywhere else in this paper unless otherwise stated. Moreover, the effect  
126 of body weight was excluded by normalising the forces [15,16] to 750 N before they were used in the  
127 analysis presented.

## 128 **2.2 Resonant and transient vibration responses**

129 Depending on the natural frequency ( $f_n$ ) of the first vibration mode, the vibration response due to human  
130 walking excitation can take three distinct shapes (**Fig. 2**):

- 131 • When the fundamental frequency is relatively small (i.e.  $f_n < 8-10$  Hz) and close to one of the  
132 integer multiples of the pacing rate ( $f_p$ ), a resonant build-up response is likely to occur (**Fig.**  
133 **2a**).
- 134 • If the fundamental frequency is much higher than the pacing rate (i.e.  $f_n \gg f_p$ ) a transient  
135 response will dominate the vibration response (**Fig. 2c**).
- 136 • When the fundamental frequency lies between the two above mentioned ranges, the sharp  
137 transient decays are reduced considerably, and the overall vibration levels are increased (**Fig.**  
138 **2b**).

139 This paper focuses on modelling the transient vibration response (**Fig. 2c**), which is the typical case for  
140 high-frequency floors.

141 Besides the natural frequency, the behaviour of the vibration response is affected by the harmonics of  
142 the walking force that excite the dominant vibration modes of the structure [26,27]. The common  
143 knowledge is that a build-up of the resonant response is unlikely to occur if the fundamental frequency

144 is higher than three or four integer multiples of the pacing rate [26,27]. The normalised Fourier  
145 amplitudes of all the forces in the database [15,16], for a length of 20.48 s, are overlapped in **Fig. 3** with  
146 a logarithmic scale in its vertical axis. There is no apparent sign that beyond, say, 10 Hz (see **Table 1**)  
147 the Fourier amplitudes of the harmonics do not exist and cannot produce a resonant build-up response.  
148 They are smaller in amplitude, but they definitely exist at integer multiples of the pacing rate.

149 To assess the effect of the harmonics of the walking excitation on the vibration response, each walking  
150 force from the database was applied to a series of SDOF oscillators, which had natural frequencies  
151 between 1-40 Hz with an increment of 0.1 Hz. Therefore, the total number of the oscillators is 391 and  
152 the total number of simulated vibration responses is 279,565. The modal mass was assumed 1 kg and  
153 the damping ratio was assumed 3% in all simulations. The duration of each simulation is equal to the  
154 length of the corresponding walking force time history, while the integration time step is 0.005 s. For  
155 the response of each simulation, the running 1-second root mean square (1-s RMS) was calculated as  
156 described in Eq. (1).

$$v_{RMS} = \sqrt{\frac{1}{T} \int_0^T v^2(t) dt} , \quad (1)$$

157 where  $v_{RMS}$  is the velocity 1-s RMS (m/s) and  $T$  is the duration of the averaging (1-s).

158 The maximum transient vibration value (MTVV), which is equal to the maximum 1-s RMS,  
159 corresponding to each simulation was used for comparison, as shown in **Fig. 4**. The grey colour  
160 represents the MTVV velocity corresponding to each walking force and varying SDOF natural  
161 frequencies, while the black colour represents the average MTVV velocity at each SDOF natural  
162 frequency.

163 The MTVV velocity is relatively high at integer multiples of pacing rates (**Fig. 4**). This is the case even  
164 for the oscillators, with a natural frequency of up to 30 Hz. Therefore, there is no evidence that the  
165 harmonics of walking forces, which correspond to frequencies above the reported cut-off frequency in

166 the design guidelines (**Table 1**), cannot induce a resonant build-up response. This implies that a more  
167 detailed study should be carried out to derive the cut-off frequency, as elaborated in the next section.

### 168 **2.3 Determining cut-off frequency between low- and high-frequency floors**

169 As already observed above, a typical transient response due to walking comprises a series of velocity  
170 peaks corresponding to heel strikes, followed by a decaying vibration response to around zero before  
171 the beginning of the next footfall, as shown in **Fig. 2c** [14]. This means that the response due to previous  
172 footfalls has a negligible contribution to the response due to the present footfall. On the other hand, for  
173 non-transient vibration responses (**Fig. 2a** and **Fig. 2b**), the response is affected by a number of previous  
174 footfalls depending on the structural damping.

175 Theoretically speaking, a transient response time history can be reconstructed from the peak responses  
176 followed by an exponentially decaying response in between them. In this case, the reconstructed  
177 vibration response level is similar to that of the original time history response (**Fig. 5**). Therefore, the  
178 proposed methodology to identify the cut-off frequency is as follows:

- 179 • Simulate vibration responses by applying measured walking forces [15,16] on SDOF oscillators  
180 with different natural frequencies.
- 181 • For each response time history, extract the peak velocity responses corresponding to each  
182 footfall strike with their exact times.
- 183 • Use the peak velocities to reconstruct the time history response which comprises only a  
184 decaying response after each peak velocity, as shown in **Fig. 5**.
- 185 • Establish the difference between the original and the reconstructed responses by calculating the  
186 ratio of their MTVVs (i.e. MTVV velocity of the reconstructed response over that for the  
187 original response).
- 188 • Repeat this process for the different natural frequencies of the SDOF oscillator and the  
189 measured walking forces [15,16].
- 190 • Identify the frequency corresponding to a value of the MTVV ratio which is reasonably close  
191 to 1.0, as explained below.



192 The closer the MTVV ratio to 1.0, the more similar are the reconstructed response and its corresponding  
193 simulated transient response. **Fig. 6** compares two cases when the MTVV ratio is close or far from 1.0.  
194 The process of generating reconstructed vibration responses was repeated for all available walking  
195 forces [15,16] when the natural frequency of the SDOF oscillator is an integer multiple of the pacing  
196 rate (up to 20 Hz). This is to consider the effect of the harmonics at these frequencies. The damping  
197 ratio used in the simulations was 3% while the modal mass was assumed 1 kg. The MTVV ratios  
198 corresponding to this analysis are presented as box plots in **Fig. 7**. The upper and lower ends of the  
199 rectangles represent the values corresponding to a 75% and 25% chance of non-exceedance,  
200 respectively. The whiskers (ends of the extended lines from the boxes) represent the maximum and  
201 minimum values.

202 At relatively low pacing rates, the MTVV ratio approaches 1.0 at a lower SDOF natural frequency than  
203 that for higher pacing rates (**Fig. 7**). This indicates the dependency of the cut-off frequency on the  
204 pacing rates. For natural frequencies at or above 14 Hz, the median of the MTVV ratios for all pacing  
205 rates (horizontal lines in the middle of the rectangles in **Fig. 7**) were within 10% of 1.0 (i.e. 0.90-1.10),  
206 which is reasonably close to 1.0. This implies that the shape of vibration responses corresponding to  
207 SDOF oscillators with natural frequencies above 14 Hz resemble typical transient responses regardless  
208 of the pacing rate. The harmonics of walking forces [15,16] corresponding to frequencies above 14 Hz  
209 are more likely to increase the amplitude of the vibration responses rather than to induce a clear resonant  
210 build-up response. Therefore, this frequency has been selected as the cut-off frequency above which the  
211 human-induced vibration of floors is dominated by transient response.

### 212 **3 Modelling human-induced vibrations of high-frequency structures**

213 This section starts with necessary details of Arup's deterministic force model (Section 3.1), followed  
214 by its expansion into a more sophisticated probability-based successor proposed in this study  
215 (Section 3.2 and Section 3.3) and its implementation in vibration serviceability assessment of high-  
216 frequency floors (Section 3.4).

### 217 3.1 Arup's model

218 The model was derived using a database of over 800 single footfalls recorded for 40 individuals stepping  
219 on a force plate while walking at a range of pacing rates controlled by a metronome [25]. The measured  
220 footfalls were shifted repeatedly along the time axes to synthesise the corresponding artificial and  
221 perfectly periodic force time history (**Fig. 8**). Each such force was applied to a series of SDOF  
222 oscillators with natural frequencies of 10-40 Hz and only the peak velocity for each simulation was  
223 extracted. The modal mass was assumed 1 kg for all simulations, so that the peak velocity response was  
224 numerically equivalent to the impulse represented by the shaded area in **Fig. 8** and expressed in Ns.  
225 Such an impulse is termed *effective impulse*.

226 For varying pacing rates, the mean of the extracted effective impulses are shown in **Fig. 9** as a function  
227 of the 'floor frequency (Hz)', which is the natural frequency of the 1 kg SDOF system. The  
228 corresponding curve fit is:

$$I_{eff} = A \frac{f_p^{1.43}}{f_n^{1.3}}, \quad (2)$$

229 where,  $I_{eff}$  is the effective impulse (Ns),  $f_p$  is the pacing rate (Hz),  $f_n$  is the SDOF natural frequency  
230 (Hz) and  $A$  is a coefficient which has a mean value of 42 and a standard deviation of 0.4 while its  
231 corresponding design value for 75% chance of non-exceedance is 54.

232 This effective impulse is used in Eq. (3) to calculate the contribution of the time history response of  
233 each vibration mode in the total response. This response corresponds to one footfall strike.

$$v_n(t) = u_i u_j \frac{I_{eff}}{M_n} e^{-\zeta_n \omega_n t} \sin(\omega_n t), \quad (3)$$

234 Here,  $v_n(t)$  (m/s) is the contribution to the velocity response from mode  $n$  at each time step  $t$ ,  $u_i$  and  
235  $u_j$  are the mode shape amplitude at the node of application of the force and the node of interest,

236 respectively,  $M_n$  (kg) is the modal mass of the mode  $n$ ,  $\zeta_n$  is the modal damping ratio,  $\omega_n$  and  $\omega_{nd}$   
237 (rad/s) are the angular frequency and damped angular frequency of mode  $n$ , respectively.

238 The contribution of each mode in the total response, calculated using Eq. (3), should be determined  
239 individually for  $N$  vibration modes with a natural frequency up to twice the fundamental frequency.

240 The total velocity response  $v_t(t)$  is calculated using Eq. (4) based on the assumption that the structure  
241 remains linear during vibration, and therefore, the principle of superposition applies.

$$v_t(t) = \sum_{n=1}^N v_n(t) \quad , \quad (4)$$

242 The criterion of the vibration serviceability assessment for high-frequency floors is based on the  
243 maximum 1-s RMS of the total response calculated using Eq. (1).

### 244 **3.2 Improved modelling procedure**

245 Based on the analysis presented in Section 2, the key differences between the steps followed to derive  
246 Arup's model and its advanced version explained in the following sections are:

- 247 • The range of natural frequencies of the SDOF oscillators used to derive the present model is  
248 14-40 Hz with an increment of 0.1 Hz, compared with 10-40 Hz used to derive Arup's model.  
249 This is to account for the proposed cut-off frequency of 14 Hz (Section 2.3).
- 250 • In the new model, SDOF simulations, which utilised continuously measured treadmill forces  
251 [15,16], were carried out to extract the peak velocities corresponding to 50 successive footfalls.  
252 These peak velocities are treated as the effective impulse ( $I_{eff}$ ) explained in Eq. (3) but they  
253 belong to the improved model presented in this paper.
- 254 • Contrary to Arup's model, the damping effect is considered in the new model. This is to take  
255 into account the slight amplification of the vibration response of high-frequency floors induced  
256 by the near-resonance effects corresponding to the higher harmonics of walking loading, as  
257 explained in Section 2.

258 Apart from the above mentioned differences, the new model was derived using the same procedure as  
259 that used for Arup’s model. The damping ratio was assumed 3% in the SDOF simulations, while the  
260 effect of other damping ratios is elaborated in Section 3.3.3. A time step of 0.005 s was used in the  
261 analysis. The total number of the peak velocities (effective impulses) obtained from the analysis is more  
262 than 900,000, i.e. 715 continuously measured walking forces [15,16], each comprising 50 footfalls,  
263 applied to 261 SDOF oscillators with natural frequencies in the range 14-40 Hz and 0.1 Hz increments.

### 264 **3.3 Formulation of the effective impulse**

265 The peak velocities corresponding to a single footfall and multiple SDOF oscillators can be presented  
266 as a spectrum. **Fig. 10** shows an example of this spectrum corresponding to one footfall within a  
267 continuous walking force, with a pacing rate of 2.25 Hz. For example, for this pacing rate there are 28  
268 continuously measured walking force time histories in the database [15,16], each having 50 footfalls.  
269 This means there are 1,400 spectra created and analysed for this pacing rate. The differences between  
270 these spectra can be explained by the inter- and intra-subject variabilities of human walking forces  
271 (Section 2.1). Hence, a statistical approach is utilised here to model the spectra as a function of SDOF  
272 natural frequency, pacing rate and damping ratio.

273 In **Fig. 10** peaks can be noticed around integer multiples of the pacing rate due to resonance or near-  
274 resonance effects. This can be explained by the effect of harmonics of the walking excitation at integer  
275 multiples of pacing rates as explained in Section 2.2.

276 To simplify the modelling of the spectrum shown in **Fig. 10**, it was split into two components: a ‘base  
277 curve’ and an ‘amplification factor’ (grey curve and black dots, respectively, in **Fig. 10**). The base curve  
278 was assumed continuous across all SDOF frequencies, while the amplification factor was assumed to  
279 be present at locations of each integer multiple of the pacing rate (black dots in **Fig. 10**). The grey dots  
280 represent the locations where the amplification factor has no effect and its location is assumed to be in  
281 the middle of each two successive integer multiples of pacing rate (subsequent pairs of the black dots).  
282 Between black and grey dots, the amplification factor can be assumed to change linearly and its value  
283 can be interpolated between them.

284 Hence, the peak velocity at each integer multiple of the walking frequency is theoretically equal to the  
 285 base curve value at that natural frequency multiplied by the corresponding contribution of the  
 286 amplification factor at the same natural frequency, as shown in **Fig. 10**.

287 A Matlab script was written to extract the amplification factor around each integer multiple of the pacing  
 288 rate, while the base curve was constructed by connecting the grey dots linearly (**Fig. 10**). The base curve  
 289 values  $B(f_n, f_p)$  (m/s) and amplification factor  $A_f(f_n, f_p)$  (dimensionless parameter) were assumed as  
 290 functions of both the natural ( $f_n$ ) and pacing ( $f_p$ ) frequencies. Hence, the effective impulse can be  
 291 mathematically described in Eq. (5).

$$I_{eff} = B(f_n, f_p) A_f(f_n, f_p) P_\zeta(f_p, f_n, \zeta) , \quad (5)$$

292 where,  $P_\zeta(f_p, f_n, \zeta)$  is the damping factor (dimensionless parameter), which is described in Section  
 293 3.3.3.

294 In the remaining part of this section, the probability distributions used to fit  $B(f_n, f_p)$  and  $A_f(f_n, f_p)$   
 295 were chosen based on the Bayesian Information Criterion [28] and the parameter fitting is based on the  
 296 Nonlinear Least Squares method [29].

### 297 3.3.1 Base curve

298 **Fig. 11** shows that  $B(f_n, f_p)$  values fit well a gamma distribution defined as [30]:

$$f(B(f_n, f_p)) = \frac{B(f_n, f_p)^{k-1} e^{-\frac{B(f_n, f_p)}{\theta}}}{\theta^k \Gamma(k)} , \quad (6)$$

299 where  $f(B(f_n, f_p))$  is the probability density function,  $k$  and  $\theta$  are the shape and scale parameters and  
 300  $\Gamma(k)$  is the gamma function evaluated at  $k$ .

301 The fitting process is repeated for 35,750 spectra (i.e. 715 walking force time histories, each comprising  
 302 50 footfalls). Values of the extracted parameters  $k$  and  $\theta$  (dimensionless parameters) were then surface  
 303 fitted as functions of  $f_n$  and  $f_p$  (measured in Hz) using polynomial and exponential forms, due to the  
 304 shape of the data to be fitted. The fitting is shown in **Fig. 12** and described by Eqs. (7) and (8).

$$k = 4.5 - 0.12 f_n + 3 f_p , \quad (7)$$

$$\theta = 0.08 + 2 \frac{f_p^{3.3}}{f_n^{1.58}} , \quad (8)$$

### 305 3.3.2 Amplification factor

306 Values of amplification factors  $A_f(f_n, f_p)$  follow the generalised extreme value distribution (**Fig. 13**),  
 307 which probability density function  $f(A_f(f_n, f_p))$  is characterised by location  $\mu$ , scale  $\sigma$  and shape  $\tau$   
 308 parameters as described in Eq. (9) [31].

$$f(A_f(f_n, f_p)) = \frac{1}{\sigma} \tau \left[ 1 + \tau \left( \frac{A_f(f_n, f_p) - \mu}{\sigma} \right) \right]^{-1-1/\tau} e^{\{-[1+\tau(\frac{A_f(f_n, f_p) - \mu}{\sigma})]^{-1/\tau}\}} \quad (9)$$

309 The extreme probability distribution is fitted to all 35,750 spectra. The extracted values of  $\mu$ ,  $\sigma$  and  $\tau$   
 310 (dimensionless parameters) are further fitted to surfaces as functions of  $f_n$  and  $f_p$  (measured in Hz). The  
 311 results are illustrated in **Fig. 14** and the mathematical formulation is described by Eqs. (10)-(12). Note  
 312 that due to the shape of the fitting data, the exponential form best fitted  $\mu$  and  $\sigma$  surfaces, while the  
 313 polynomial function best fitted  $\tau$  values.

$$\mu = 0.98 + 7.6 \frac{f_p^{2.5}}{f_n^{1.82}} , \quad (10)$$

$$\sigma = -0.03 + 0.85 \frac{f_p^{1.3}}{f_n} , \quad (11)$$

$$\tau = 0.18 - 0.00013 f_n^2 - 0.015 f_n f_p + 0.0004 f_p f_n^2 , \quad (12)$$

314 Interpolation of  $A_f(f_n, f_p)$  should be considered if the natural frequency is not an integer multiple of the  
 315 pacing rate (**Fig. 10**). For instance, if the natural frequency lies exactly in the middle of two successive  
 316 integer multiples of the pacing rate, the amplification factor will have no effect on the response (i.e.  
 317  $A_f(f_n, f_p) = 1.0$ ). This takes into account that the amplification factor has a reduced effect between the  
 318 integer multiples of the pacing rate, as shown in **Fig. 10**.

### 319 3.3.3 Damping effect

320 A damping factor is developed in this section to scale amplification factor  $A_f(f_n, f_p)$  to account for the  
 321 effect of a floor near-resonance with the harmonics of walking excitation above 14 Hz and to account  
 322 for damping ratios  $\zeta$  of the SDOFs different from 3%. Hence, the numerical simulations presented in  
 323 the previous section are repeated here to derive amplification factors  $A'_f(f_n, f_p, \zeta)$  for damping ratios in  
 324 the range 0.5%-6%, with an increment of 0.1%. The damping factor  $P_\zeta(f_p, f_n, \zeta)$  can be expressed as:

$$P_\zeta(f_p, f_n, \zeta) = \frac{A_f(f_n, f_p)}{A'_f(f_n, f_p, \zeta)} , \quad (13)$$

325 The plane defined by Eq. (14) is fitted to  $P_\zeta(f_p, f_n, \zeta)$  for different damping ratios:

$$P_\zeta(f_p, f_n, \zeta) = a + b f_p + c f_n , \quad (14)$$

326 where,  $a$ ,  $b$  and  $c$  are the parameters of the equation (dimensionless parameters). **Fig. 15** shows the  
 327 fitted plane corresponding to a damping ratio of 5%.

328 Finally, values of the parameters  $a$ ,  $b$  and  $c$  are curve fitted as functions of the damping ratio. The  
 329 resulting curve fits are illustrated in **Fig. 16** and described by Eqs. (15), (16) and (17). The shapes of  
 330 these equations are decided based on the trends observed in the data (**Fig. 16**).

$$a = 2.82 - 2.58 \zeta^{0.1} \quad (15)$$

$$b = -0.0174 + \frac{0.38}{e^{100\zeta}} \quad (16)$$

$$c = 0.0028 - \frac{0.0138}{e^{50\zeta}} \quad (17)$$

331 According to Eq. (14), the range of  $P_\zeta(f_p, f_n, \zeta)$  is 0.86-1.72. The lower and upper limits correspond  
 332 to  $f_p=2.5$  Hz,  $f_n=14$  Hz and  $\zeta =6\%$  and  $\zeta =0.5\%$ , respectively. It is assumed that the damping factor  
 333  $P_\zeta(f_p, f_n, \zeta)$  has the highest effect when  $f_n$  is an integer multiple of  $f_p$  due to the near-resonant effect  
 334 with the higher harmonics of walking, as was the case with  $A_f(f_n, f_p)$  in the previous section. Hence, if  
 335 the natural frequency is not an integer multiple of the pacing rate,  $P_\zeta(f_p, f_n, \zeta)$  need to be interpolated  
 336 in the same way as  $A_f(f_n, f_p)$ .

### 337 **3.4 Implementation of the new model**

338 Vibration serviceability assessment of a high-frequency floor using the new model takes the following  
 339 steps:

- 340 • The modal properties are derived from either modal testing or a finite element model (FEM) of  
 341 the floor.
- 342 • The walking path, pacing rate and its corresponding walking speed or step length can be utilised  
 343 to calculate the time that a walking person spends while walking on the floor. This is necessary  
 344 to determine the number of footfalls and the duration of the vibration response. Further  
 345 discussion about deciding an appropriate pacing rate and walking path is beyond the scope of



346 this paper. However, a reader is advised to generate value of the pacing rate based on probability  
347 density functions available in the literature [32].

- 348 • For each vibration mode, Eqs. (7), (8), (10)-(12) are used to calculate the distribution  
349 parameters related to the gamma and the generalised extreme value distributions. Random  
350 values of these distributions are generated based on Eq. (6) and (9) corresponding to  $A_f(f_n, f_p)$   
351 and  $B(f_n, f_p)$ , respectively. The number of the generated values is the same as the number of  
352 footfalls calculated above. The effect of damping is considered by calculating  $P_\zeta(f_p, f_n, \zeta)$   
353 using Eq. (14), which parameters can be calculated using Eq. (15), (16) and (17). The generated  
354 values of  $A_f(f_n, f_p)$  and  $P_\zeta(f_p, f_n, \zeta)$  need to be scaled depending on the natural frequency of  
355 the considered vibration mode and the pacing rate, as explained in Section 3.3.2 and **Fig. 10**.
- 356 • The effective impulse  $I_{eff}$  corresponding to each footfall can be determined using Eq. (5). The  
357 time history of decaying vibration response due to each effective impulse is calculated utilising  
358 Eq. (3) and the modal properties of each mode under consideration. The total time history  
359 response due to each mode can be obtained when the decaying responses are sequenced one  
360 after another to form a continuous response time history for the duration of walking. The time  
361 between each two successive footfalls needs to be consistent with the pacing rate. The residual  
362 of each decaying response at the beginning of the next footfall is assumed to be zero.
- 363 • The total response corresponding to the contribution from all vibration modes having  
364 frequencies up to twice the fundamental frequency is calculated using Eq. (4). This number of  
365 vibration modes is adopted from the Arup's model.

366 By following the above mentioned procedure, a single response time history can be obtained. To  
367 consider the statistical nature of  $A_f(f_n, f_p)$  and  $B(f_n, f_p)$ , a sufficient number of responses needs to be  
368 generated as explained below. This number of samples  $n$  is defined by Eq. (18) [33].

$$n = \left( \frac{s}{SE_{\bar{x}}} \right)^2, \quad (18)$$

369 where,  $s$  is the standard deviation of the population and  $SE_{\bar{x}}$  is the standard error of their mean.

370 In this study, the samples are a set of MTVV velocity calculated following the above mentioned  
371 procedure, while the population refers to all possible MTVV velocities. As the standard deviation of  
372 the population  $s$  is unknown, it is estimated to be the standard deviation of the samples. Assuming the  
373 samples are independent and identically distributed, there is a 95% chance that their mean is within the  
374 population mean  $\bar{x}$  a tolerance of  $1.96 SE_{\bar{x}}$  [33]. This tolerance should be specified based on the  
375 required accuracy [33]. The authors suggest using a tolerance value of 1% of the mean of the samples.

376 Hence, the sufficient number of responses can be found in an iterative approach. After generating each  
377 sample (MTVV velocity), the sufficient number of samples  $n$  can be calculated using Eq. (18) and  
378 compared with the actual number of generated samples. When Eq. (18) is fulfilled (i.e. the number of  
379 generated samples is equal or higher than the sufficient number of samples  $n$ ) the simulations can be  
380 stopped.

381 Finally, the cumulative distribution function (CDF) of the MTVV velocity, corresponding to the  
382 generated responses, can be obtained and the vibration serviceability assessment can be carried out  
383 based on the desired probability. The whole process explained in this section is summarised in **Fig. 17**.

## 384 **4 Verification**

385 The performance of the model elaborated in the previous section is verified here against numerical  
386 simulations (Section 4.3) of the vibration response calculated using the measured treadmill forces  
387 (Section 2.1) and an FEM of a high-frequency floor (Section 4.1). Simulations are also carried out  
388 using the original Arup model (Section 4.3) for comparison (Section 4.4).

### 389 **4.1 Finite element model**

390 The FEM utilised in this section is developed using ANSYS FE software [34] and is updated to match  
391 the experimentally measured modal properties of the corresponding real floor (**Fig. 18**). The floor is a  
392 58m × 14m composite slab supported by steel beams and columns. The slab has a concrete deck with

393 thickness 130 mm and it was modelled using a shell element (SHELL181 in ANSYS) assuming  
 394 isotropic behavior with a mesh size of 0.5m. BEAM188 element was used to model the supporting steel  
 395 beams and columns. The elastic modulus used to model the concrete and steel materials are 38 GPa and  
 396 210 GPa, while their corresponding Poisson's ratios are 0.2 and 0.3, respectively. The structure has a  
 397 maximum span of  $7.0 \times 6.0$  m and similar (but not identical) structural configuration between its two  
 398 wings (left and right). The columns were fixed at the far ends and the lateral movement of the floor was  
 399 restrained at the perimeter of the floor.

400 **Fig. 19** shows the first six vibration modes of the structure. While the first 18 vibration modes have  
 401 contributions from either the left or the right wing of the structure, the other eight vibration modes have  
 402 contributions from both wings. The dynamic properties of all vibration modes with a natural frequency  
 403 up to twice the fundamental frequency (26 vibration modes) were extracted from the FEM and used in  
 404 the analysis presented in the next section.

## 405 **4.2 Simulations based on measured walking forces and FEM**

406 The simulations are carried out using 60 measured forces (Section 2.1) due to people walking at six  
 407 walking frequencies (i.e. ten walking forces for each pacing rate 1.4, 1.6, 1.8, 2.0, 2.2 and 2.4 Hz)  
 408 representing slow to fast walking scenarios.

409 A walking path expected to produce the maximum response is specified before performing the  
 410 simulations (**Fig. 19**). A constant value of 0.75 m was used for the step length. Unity-scaled (normalised  
 411 to a maximum value of 1.0) mode shapes  $\{\phi_r\}$  were used to calculate the modal force time histories  
 412  $P_r(t)$  for each mode  $r$  for the walking force moving along the walking path, as described in Eq. (19):

$$P_r(t) = f(t) \phi_r(v.t) \quad , \quad (19)$$

413 where,  $f(t)$  is the physical walking force,  $t$  is time,  $v$  is the constant walking speed,  $r = 1, 2, \dots$  refers  
 414 to different modes of vibration and  $\phi_r(v.t)$  is amplitude of the mode shape  $r$  at the location of the  
 415 pedestrian at time  $t$ . Essentially Eq. (19) describes scaling of walking force  $f(t)$  by mode shape

416 amplitudes  $\phi_r(v, t)$  along the walking path. Due to the discrete locations of the nodes, the amplitudes  
417 of the unity-scaled mode shapes corresponding to the location of the pedestrian at each time step were  
418 obtained by interpolation.

419 The contribution of each mode in the total response was obtained by applying the modal force time  
420 history to a SDOF oscillator having the same modal properties as that extracted from the FEM. The  
421 Newmark integration method was used to solve the corresponding equation of motion with a time step  
422 of 0.005 s. The modal damping ratio was assumed 3% in all simulations. The vibration responses were  
423 calculated at a node which has contributions from as many vibration modes as possible (red dot in **Fig.**  
424 **19**). Hence, the contribution of each mode in the total response was multiplied by its corresponding  
425 mode shape value at that node ( $u_j$ ). The total responses were determined based on the superposition  
426 principle, i.e. by adding responses from all vibration modes having a natural frequency up to twice the  
427 fundamental frequency.

428 This procedure was repeated to simulate the vibration response due to each measured walking force.  
429 Therefore, there are 60 vibration response time histories, here called “oscillator based responses”, used  
430 in the next section for comparison with the vibration responses calculated using both the new model  
431 and Arup’s model.

### 432 **4.3 Calculated responses using the new model and Arup’s model**

433 The same walking path, pacing rates, step length and modal properties from the previous section were  
434 used here to calculate the responses, using both the newly proposed model and Arup’s model.

435 For the new model, the procedure described in Section 3.4 was followed to estimate the vibration  
436 response time histories and their corresponding MTVV velocity. After generating each response, an  
437 estimation of the required number of generated responses, according to Eq. (18), is obtained and  
438 compared with the actual number of generated responses, as shown in **Fig. 20**.

439 The vibration response using Arup’s model was estimated in a similar procedure. The main difference  
440 is that the effective impulse is calculated based on Eq. (2) instead of Eq. (5).

441 **4.4 Results and comparison**

442 Examples of velocity time history responses calculated using the oscillator based simulations and the  
443 new model are presented in **Fig. 21**. Based on the visual inspection, the responses are apparently very  
444 similar.

445 A numerical comparison between the vibration responses can be made using their cumulative  
446 probability distribution. **Fig. 22** shows the overlaid plot of the cumulative probability distribution  
447 corresponding to each vibration response time history obtained using the oscillator based simulations,  
448 the new model and Arup's model.

449 This figure shows that the vibration response levels calculated using the new model (light grey curves  
450 in **Fig. 22**) are relatively close to that obtained from the oscillator based simulations (dark grey curves  
451 in **Fig. 22**). The vibration responses calculated using Arup's model slightly overestimate the responses  
452 corresponding to the pacing rates of 1.4 Hz and 1.6 Hz, while less conservative results were obtained  
453 for vibration responses corresponding to other pacing rates (**Fig. 22**).

454 A more obvious and appropriate comparison between the considered vibration responses can be carried  
455 out using the MTVV of the velocity responses. **Fig. 23** presents the cumulative probability distribution  
456 of the MTVV velocity corresponding to the generated responses using the new model. This represents  
457 the MTVV velocity prediction range of the proposed model. For comparison purposes, the projections  
458 of the MTVV velocity, corresponding to the responses obtained using the oscillator based simulations  
459 and Arup's model, on the cumulative probability distribution in **Fig. 23** were illustrated in the same  
460 figure.

461 Most of the MTVV velocity corresponding to the oscillator based simulations are within the predicted  
462 range of the vibration responses obtained using the new model (**Fig. 23**). Only four vibration responses  
463 (out of 60) obtained from the oscillator based simulations are outside but relatively close to the predicted  
464 range of the vibration levels calculated using the new model. Ideally, the MTVV velocity of the  
465 oscillator based simulations should be clustered around vibration levels corresponding to a cumulative

466 probability distribution value of 0.5 (**Fig. 23**). This is broadly achieved by most of the simulated MTVV  
467 velocity values (dashed grey lines in **Fig. 23**).

468 Arup's methodology for vibration prediction has an implicit 75% chance of non-exceedance probability  
469 for a certain vibration level as explained in Section 3.1. This implies that the MTVV velocity  
470 corresponding to the responses obtained using Arup's model should be higher than that corresponding  
471 to seven responses (out of 10) obtained from the oscillator based simulations related to each pacing rate.  
472 By comparing these MTVV velocity values, it is obvious that the vibration levels calculated using  
473 Arup's model are significantly overestimated for low pacing rates (1.4 Hz and 1.6 Hz) and slightly  
474 underestimated for a high pacing rate (2.4 Hz). Closer vibration levels were obtained for responses  
475 corresponding to pacing rates 1.8 Hz and 2.0 Hz (**Fig. 23**). The same trend can be observed when they  
476 are compared with the MTVV velocity corresponding to the new model (**Fig. 23**).

## 477 **5 Discussion and conclusions**

478 This paper presents an improved version of Arup's approach for the vibration serviceability assessment  
479 of high-frequency floors. The main advances are the new cut-off frequency of 14 Hz rather than 10 Hz  
480 between low- and high-frequency floors and the probabilistic rather than deterministic approach to  
481 modelling individual walking loading. Note that using cut-off frequency 14 Hz in the existing models  
482 for high-frequency floors (including Arup's model) may not be appropriate, as they were developed  
483 using simulations of different oscillators than in this study.

484 Another key advantage of the proposed force model is its capability to provide probability-based  
485 vibration serviceability assessment related to any given probability of exceedance of the floor vibration  
486 levels. This is far more flexible than Arup's original model providing vibration levels corresponding to  
487 75% probability of non-exceedance. The probabilistic approach of the proposed individual walking  
488 loading and the related criterion for assessing vibration serviceability describes better the stochastic  
489 nature of human-induced vibrations than that of the existing model.

490 The simulation results showed that the new model can predict the vibration levels for more than 90%  
491 of cases. Those outside the range showed vibration levels mostly below (yet close to) their targets (**Fig.**  
492 **23**). On the other hand, Arup's model tends to overestimate the response for low pacing rates, while a  
493 slight underestimation of the responses was noticed for high pacing rates. The best performance of  
494 Arup's model was observed for pacing rates corresponding to an average walking speed (i.e. 1.8 Hz  
495 and 2.0 Hz). This is in line with previous findings that Arup's model can underestimate the response  
496 for high-frequency floors with relatively low fundamental frequency and high pacing rate [14]. The  
497 reason for this could be related to using synthetic rather than continuously measured walking forces  
498 [15,16] and the range of the SDOF frequencies used to derive the model.

499 As the new model requires repetitive simulations, vibration serviceability assessment in design practice  
500 would benefit from a computer software where the results can be obtained within a few seconds on a  
501 standard PC configuration. In future this approach could also involve in the calculations statistical  
502 treatment of walking paths and other force parameters, such as pacing rate and body weight. Finally,  
503 the new model needs to be verified against vibration serviceability surveys of real high-frequency floors  
504 when occupied by walking people.

## 505 **Acknowledgements**

506 The authors would like to acknowledge the College of Engineering, Mathematics and Physical Sciences  
507 in the University of Exeter for the financial support provided for the PhD programme of the first author.

508 The authors would also like to acknowledge the UK Engineering and Physical Sciences Research  
509 (EPSRC) for the following research grants:

- 510 • Platform Grant EP/G061130/2 (Dynamic performance of large civil engineering structures: an  
511 integrated approach to management, design and assessment) and
- 512 • Standard Grant EP/I029567/1 (Synchronization in dynamic loading due to multiple pedestrians  
513 and occupants of vibration-sensitive structures).

514

515 **References**

- 516 [1] Racic V, Pavic A. Mathematical model to generate asymmetric pulses due to human  
517 jumping. ASCE J Eng Mech 2009;1206-1211.
- 518 [2] Middleton CJ, Brownjohn JMW. Response of high frequency floors: A literature review.  
519 Engineering Structures 2010;32:337–52.
- 520 [3] BSI. UK national annex to eurocode 1: actions on structures - Part 2: traffic loads on bridges.  
521 vol. NA to BS E. British Standards Institution; 2008.
- 522 [4] Ungar EE, White RW. Footfall-induced vibrations of floors supporting sensitive equipment.  
523 Sound and Vibration 1979;10–3.
- 524 [5] Galbraith FW. Ground Loading from Footsteps. The Journal of the Acoustical Society of  
525 America 1970;48:1288. doi:10.1121/1.1912271.
- 526 [6] Amick H, Hardash S, Gillett P, Reaveley RJ. Design of Stiff, Low-Vibration Floor Structures.  
527 Proceedings of International Society for Optical Engineering, vol. 1619. San Jose, San Jose,  
528 CA: SPIE; 1991, p. 180–91.
- 529 [7] Murray TM, Allen DE, Ungar EE. Floor Vibrations Due to Human Activity - AISC DG11.  
530 vol. DG-11. 1st ed. American Institute of Steel Construction; 1997.
- 531 [8] Fanella DA, Mota M. Design Guide for Vibrations of Reinforced Concrete Floor Systems.  
532 First Edit. CRSI; 2014.
- 533 [9] Wyatt TA, Dier AF. Building in steel, the way ahead. International Symposium: Building in  
534 Steel, The Way Ahead 1989.
- 535 [10] Wyatt TA. Design Guide on the Vibration of Floors SCI P076. London: The Steel  
536 Construction Institute, Construction Industry Research and Information Association; 1989.



- 537 [11] Hanagan LM, Murray TM. Active Control Approach for Reducing Floor Vibrations. Journal  
538 of Structural Engineering 1997;123:1497–505. doi:10.1061/(ASCE)0733-  
539 9445(1997)123:11(1497).
- 540 [12] Liu D, Davis B. Walking Vibration Response of High-Frequency Floors Supporting Sensitive  
541 Equipment. Journal of Structural Engineering 2014;4014199-1-04014199–10.  
542 doi:10.1061/(ASCE)ST.1943-541X.0001175.
- 543 [13] Ellis BR, Ji T, Littler JD. The response of grandstands to dynamic crowd loads. Proceedings of  
544 ICE: Structures and Buildings 2000;140:355–65.
- 545 [14] Brownjohn JMW, Middleton CJ. Procedures for vibration serviceability assessment of high-  
546 frequency floors. Engineering Structures 2008;30:1548–59.
- 547 [15] Racic V, Brownjohn JMW. Mathematical modelling of random narrow band lateral excitation  
548 of footbridges due to pedestrians walking. Computers & Structures 2012;90–91:116–30.  
549 doi:10.1016/j.compstruc.2011.10.002.
- 550 [16] Racic V, Brownjohn JMW. Stochastic model of near-periodic vertical loads due to humans  
551 walking. Advanced Engineering Informatics 2011;25:259–75. doi:10.1016/j.aei.2010.07.004.
- 552 [17] Brownjohn JMW, Pavic A, Omenzetter P. A spectral density approach for modelling  
553 continuous vertical forces on pedestrian structures due to walking. Canadian Journal of Civil  
554 Engineering 2004;31:65–77. doi:10.1139/103-072.
- 555 [18] Živanovic S, Pavic A. Probabilistic Modeling of Walking Excitation. Journal of Constructional  
556 Steel Research 2009;23:132–43.
- 557 [19] Brownjohn JMW, Racic V, Chen J. Universal response spectrum procedure for predicting  
558 walking-induced floor vibration. Mechanical Systems and Signal Processing 2015:1–15.  
559 doi:10.1016/j.ymsp.2015.09.010.

- 560 [20] Willford MR, Young P. Improved methodologies for the prediction of footfall-induced  
561 vibration. Proceedings of the Sixth European Conference on Structural Dynamics EURODYN  
562 2005.
- 563 [21] Willford MR, Young P, Field C. Predicting footfall-induced vibration: Part 2. Structures &  
564 Buildings 2007;160:73–9.
- 565 [22] Pavic A, Reynolds P, Prichard S, Lovell M. Evaluation of mathematical models for predicting  
566 walking-induced vibrations of high-frequency floors. International Journal of Structural  
567 Stability and Dynamics 2003;3:107–30. doi:10.1142/S0219455403000756.
- 568 [23] Ohlsson S V. Floor Vibrations and Human Discomfort. Chalmers University of Technology,  
569 1982.
- 570 [24] Eriksson P-E. Vibration of low-frequency floors - dynamic forces and response prediction  
571 1994.
- 572 [25] Kerr SC. Human induced loading on staircases. PhD Thesis. University College London,  
573 Mechanical Engineering Department, London, UK, 1998.
- 574 [26] Murray TM, Allen DE, Ungar EE, Davis DB. Vibrations of Steel-Framed Structural Systems  
575 Due to Human Activity: AISC DG11 Second Edition. 2016.
- 576 [27] Pavic A, Willford MR. Vibration Serviceability of Post-tensioned Concrete Floors - CSTR43  
577 App G. Appendix G in Post-Tensioned Concrete Floors Design Handbook - Technical Report  
578 43 2005:99–107.
- 579 [28] Schwarz G. Estimating the Dimension of a Model. The Annals of Statistics 1978;6:461–4.  
580 doi:10.1214/aos/1176344136.
- 581 [29] Teunissen PJG. Nonlinear least squares. Manuscripta Geodaetica 1990;15:137–50.
- 582 [30] Scheaffer R, McClave J, Franklin C. Probability and statistics for engineers. Fifth edit. Boston,

583 MA, USA: Cengage Learning; 2010.

584 [31] Kotz S, Nadarajah S. Extreme value distributions. 2000. doi:10.1007/978-3-642-04898-2.

585 [32] Racic V, Pavic A, Brownjohn JMW. Experimental identification and analytical modelling of  
586 human walking forces: Literature review. *Journal of Sound and Vibration* 2009;326:1–49.  
587 doi:10.1016/j.jsv.2009.04.020.

588 [33] Rothrock L, Narayanan S. *Human-in-the-Loop Simulations, Methods and Practice*. London:  
589 Springer; 2011. doi:10.1007/978-0-85729-883-6.

590 [34] ANSYS Inc. ANSYS® Academic Research, Release 14.5 2015.

591 [35] Willford MR, Field C, Young P. Improved methodologies for the prediction of footfall-  
592 induced vibration. *Architectural Engineering Conference, Omaha, Nebraska, United States:*  
593 2006. doi:10.1061/40798(190)17.

594 [36] Ohlsson S V. Ten Years of Floor Vibration Research - A Review of Aspects and Some  
595 Results. In: *Proceedings of the Symposium/Workshop on Serviceability of Buildings*  
596 *(Movements, Deformations, Vibrations)*, vol. 1, Ottawa, Canada: 1988, p. 419–34.

597 [37] Allen DE, Murray TM. Design criterion for vibrations due to walking. *Engineering Journal*  
598 *AISC* 1993;30:117–29.

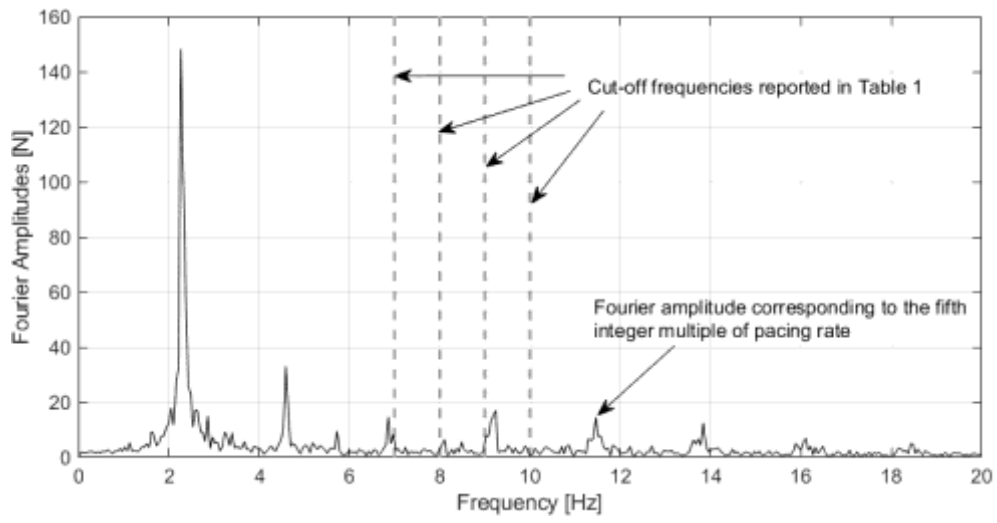
599 [38] Willford MR, Young P. *A Design Guide for Footfall Induced Vibration of Structures - CCIP-*  
600 *016*. Slough: The Concrete Centre; 2006.

601 [39] Smith AL, Hicks SJ, Devine PJ. *Design of floors for vibration - A new approach SCI P354,*  
602 *Revised Ed. vol. SCI P354*. The Steel Construction Institute; 2009.

603

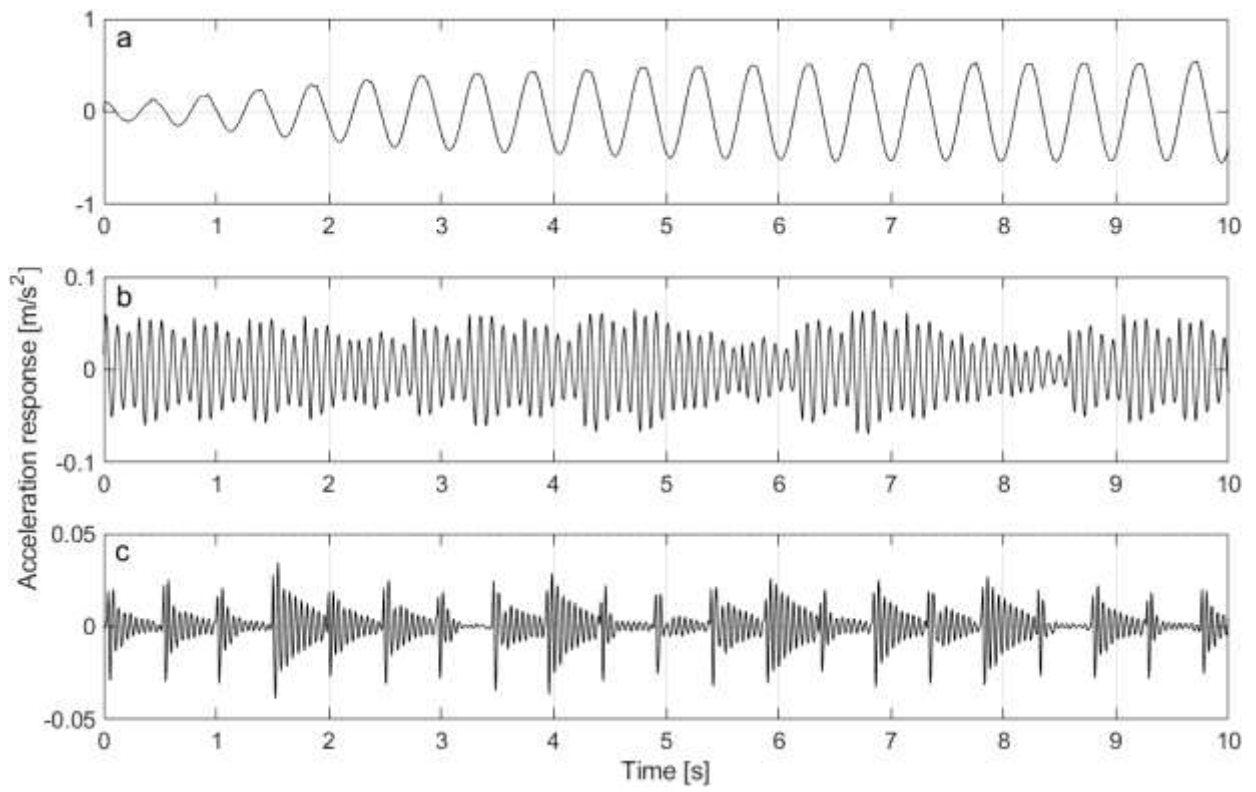
604

605 **Figures**



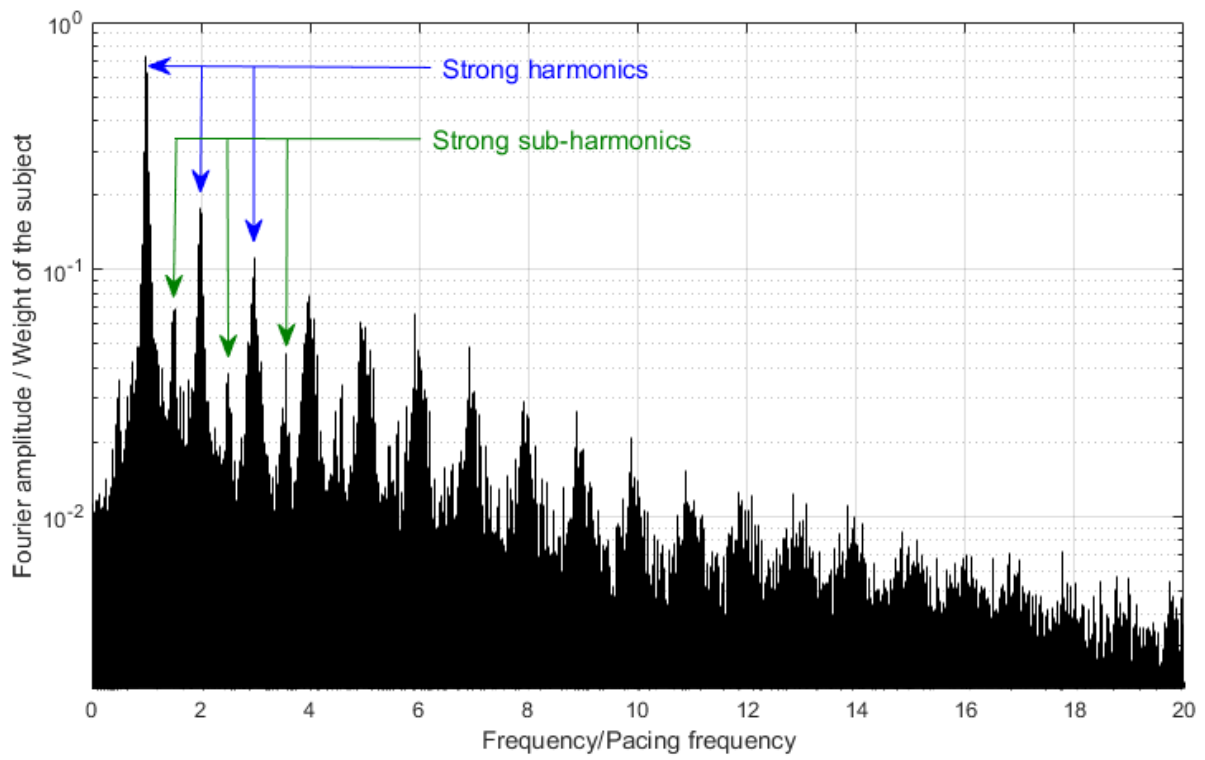
606

607 **Fig. 1.** Fourier amplitudes of a walking force signal measured using an instrumented treadmill corresponding to  
608 a pacing rate of 2.3 Hz.



609

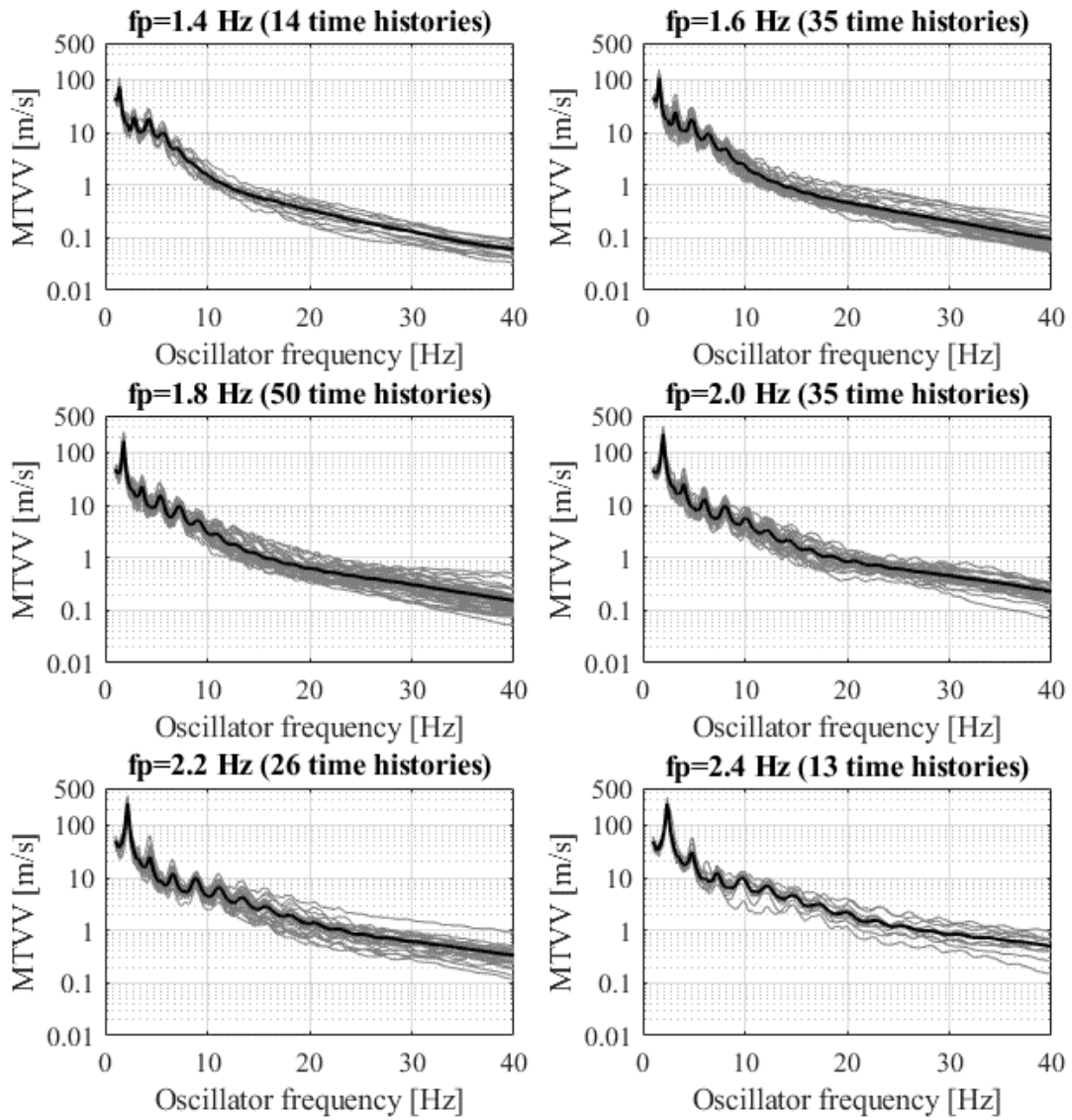
610 **Fig. 2.** Simulated vibration responses due to a recorded walking force with  $f_p=2.0$  Hz and natural frequency of  
 611 the oscillator (a)  $f_n=2.0$  Hz, (b)  $f_n=10$  Hz and (c)  $f_n=20$  Hz.



612

613 **Fig. 3.** Normalised Discrete Fourier amplitudes for all available walking forces [15,16] with pacing rates

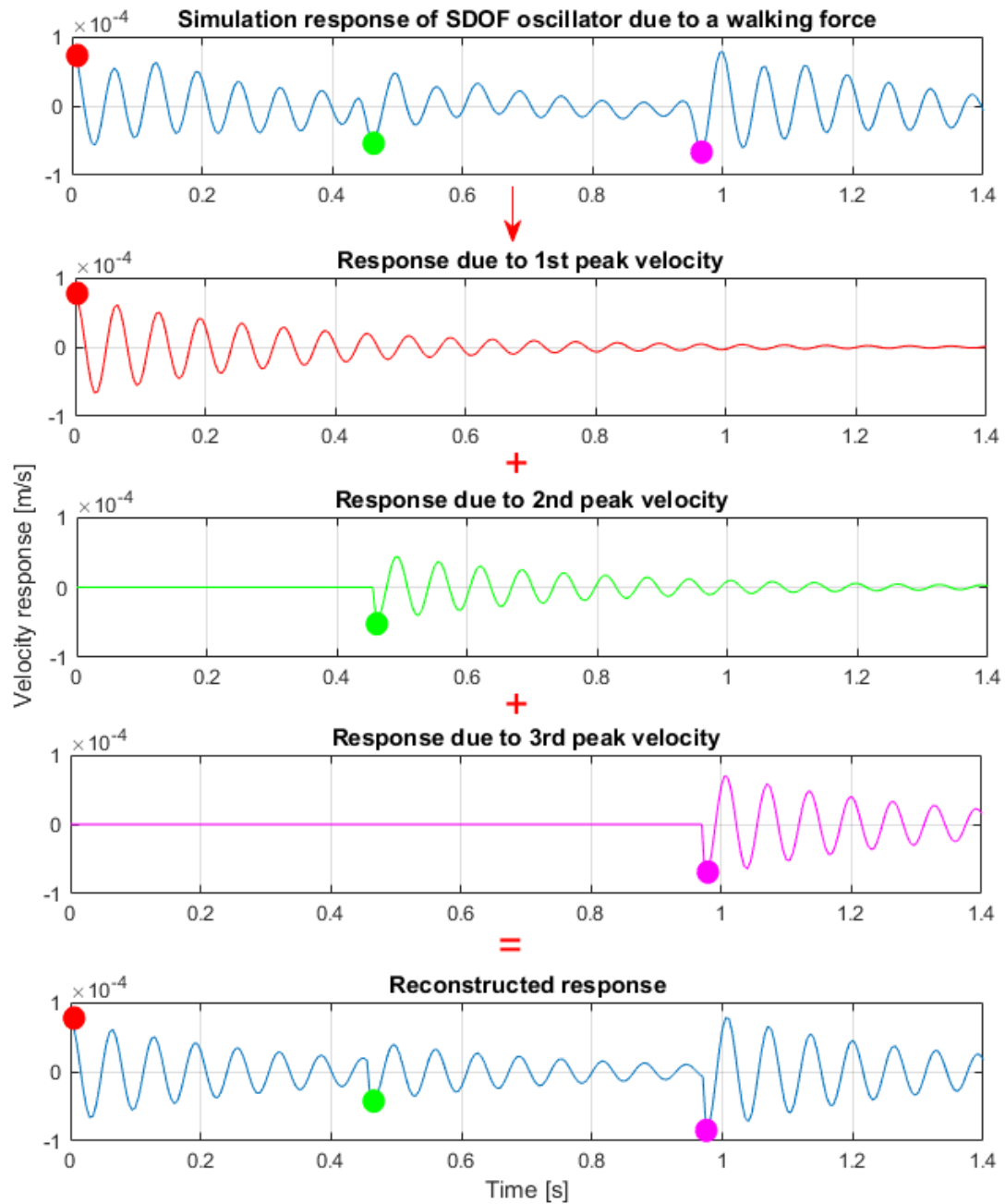
614 between 1.4-2.5 Hz.



615

616 **Fig. 4.** MTVV velocity (grey) for pacing rates ( $f_p$ ) from 1.4 Hz (up left) to 2.4 Hz (bottom right). Black

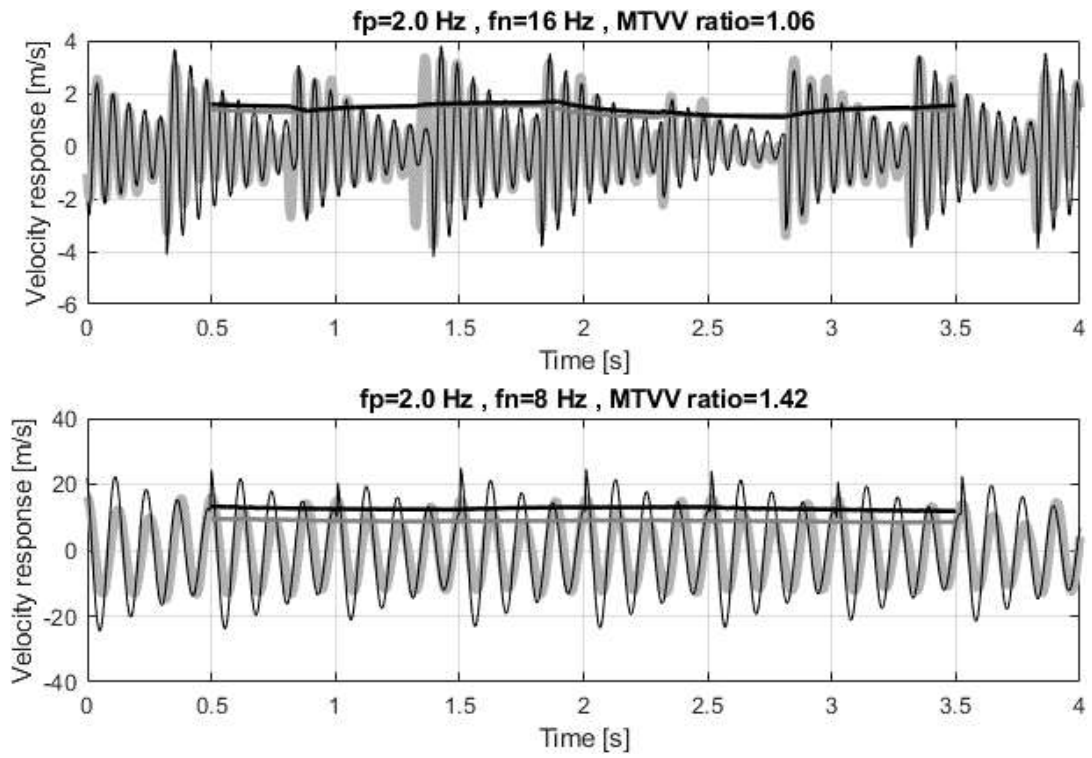
617 represents the average MTVV velocity at each natural frequency.



618

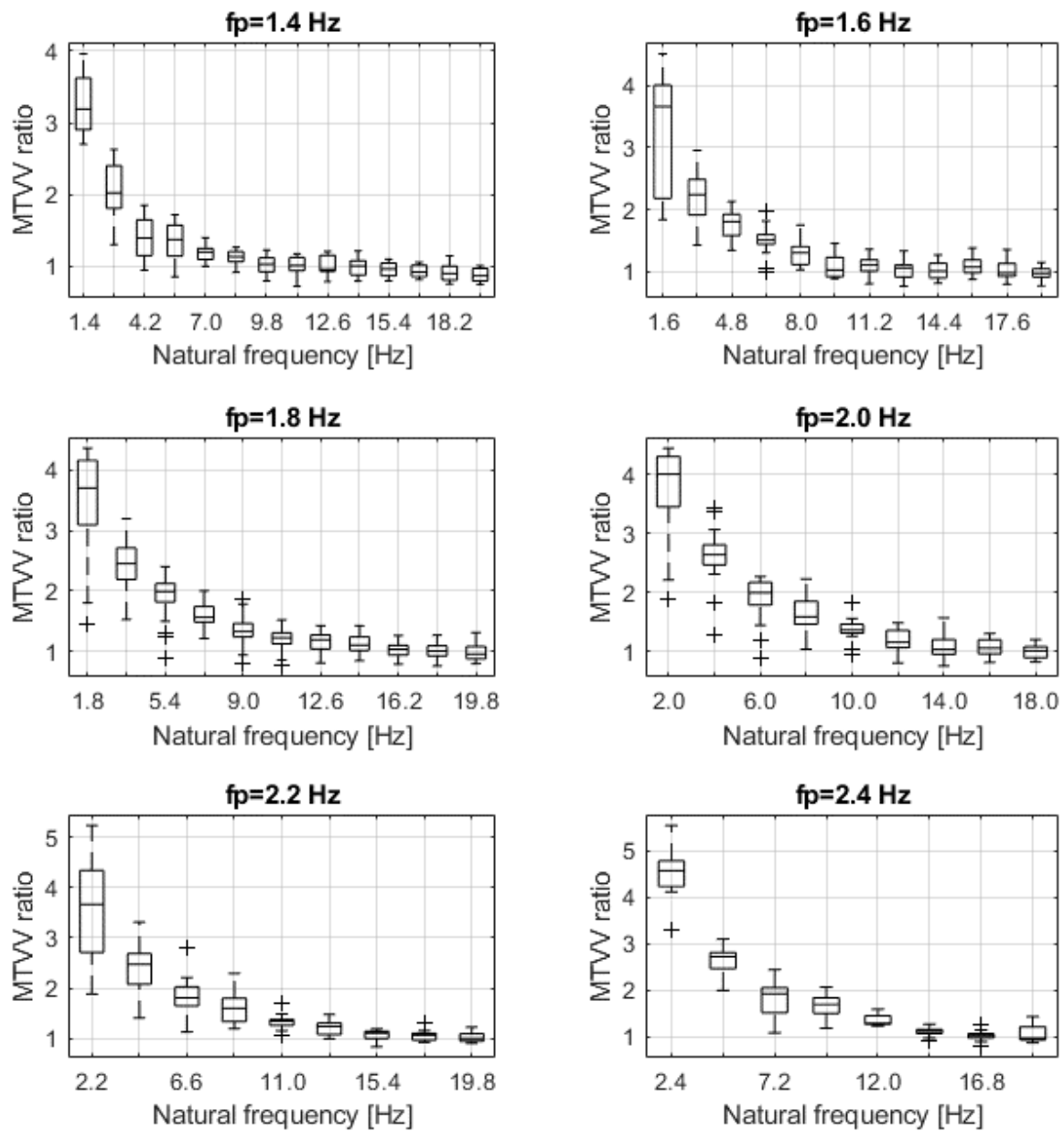
619 **Fig. 5.** Typical reconstructed vibration response from simulation of a walking force with pacing rate ( $f_p$ ) of 2.0  
 620 Hz applied on SDOF oscillator with a natural frequency ( $f_n$ ) of 16 Hz. Red, green and pink dots refer to the 1<sup>st</sup>,  
 621 2<sup>nd</sup> and 3<sup>rd</sup> peak velocities, respectively.





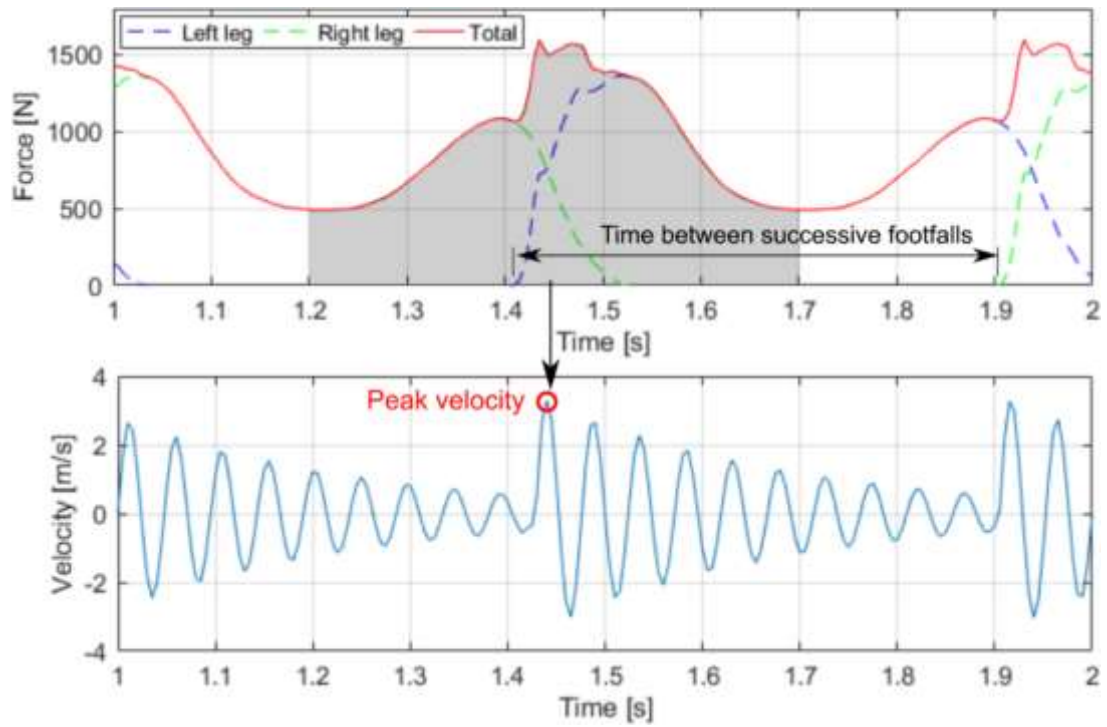
622

623 **Fig. 6.** Comparison between simulated (grey) and reconstructed (black) vibration responses with their  
 624 corresponding 1-s running RMS for natural frequency ( $f_n$ ) of 16 Hz (top) and 8 Hz (bottom).



625

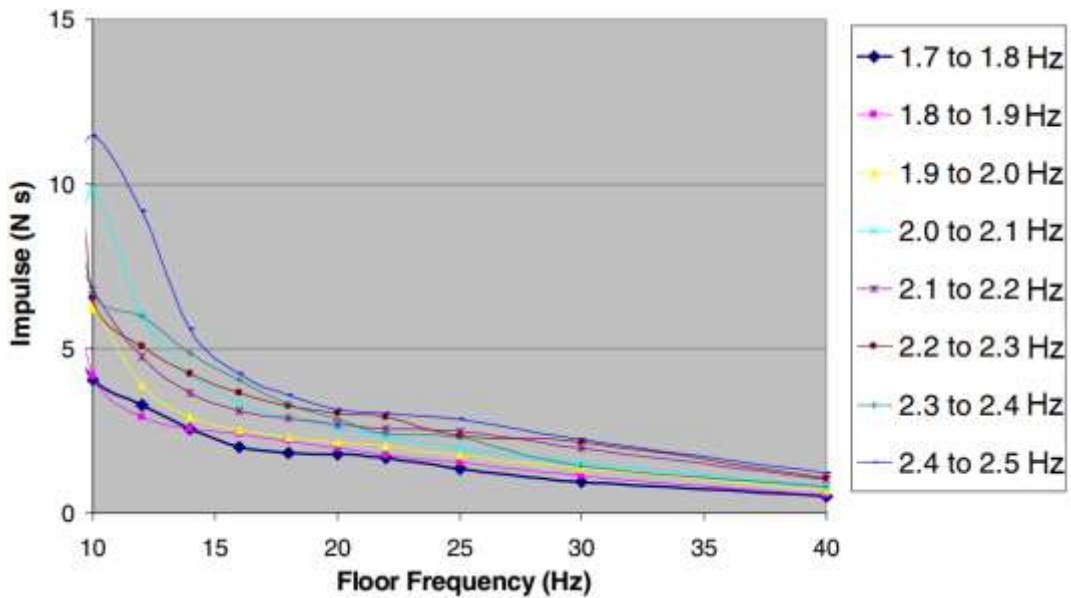
626 **Fig. 7.** MTWV ratio between simulated and reconstructed vibration responses at different pacing rates ( $f_p$ ).



627

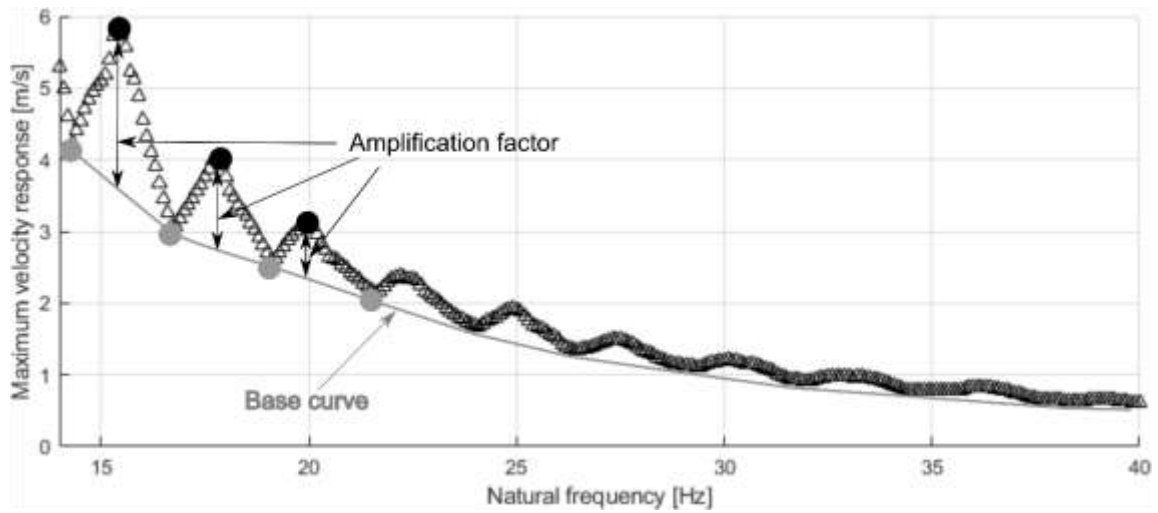
628 **Fig. 8.** Arup's approximation of the typical walking force (top) and its corresponding velocity vibration  
 629 response (bottom).

630



631

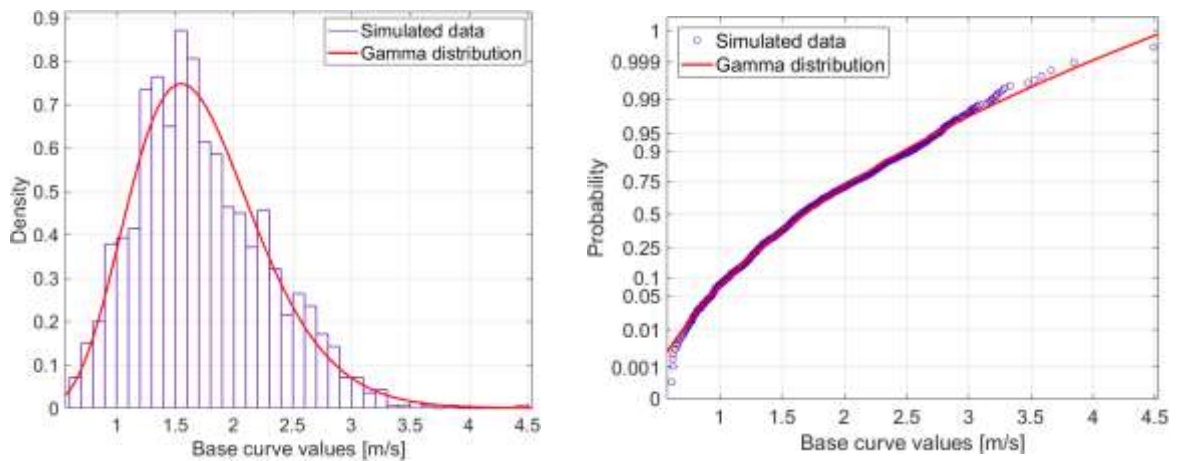
632 **Fig. 9.** Effective impulse derived from Kerr [25] footfall traces (after Willford et al. [35]).



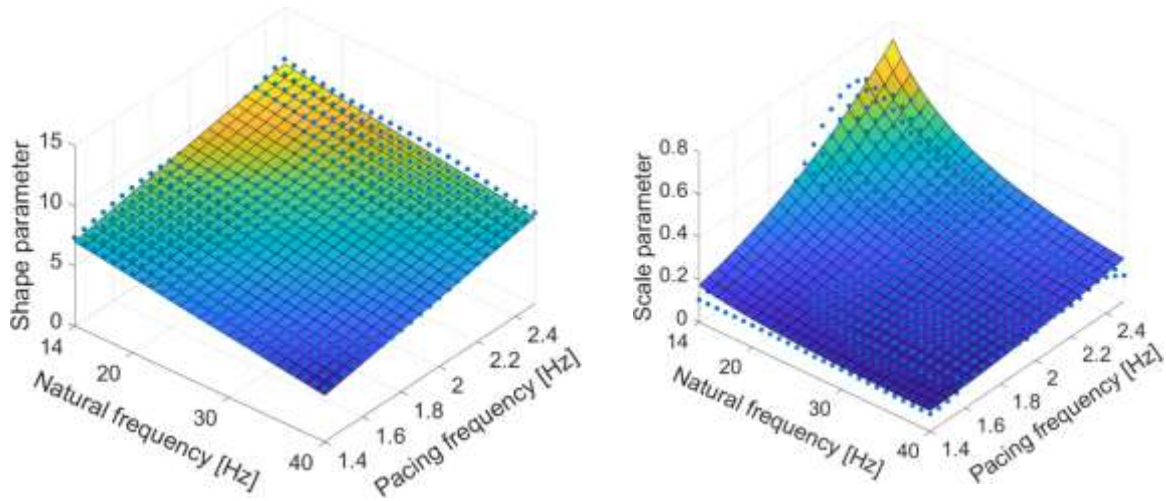
633

634 **Fig. 10.** Spectrum (black triangles) of peak velocity response corresponding to one footfall within a continuous  
 635 walking force with a pacing rate of 2.25 Hz.

636

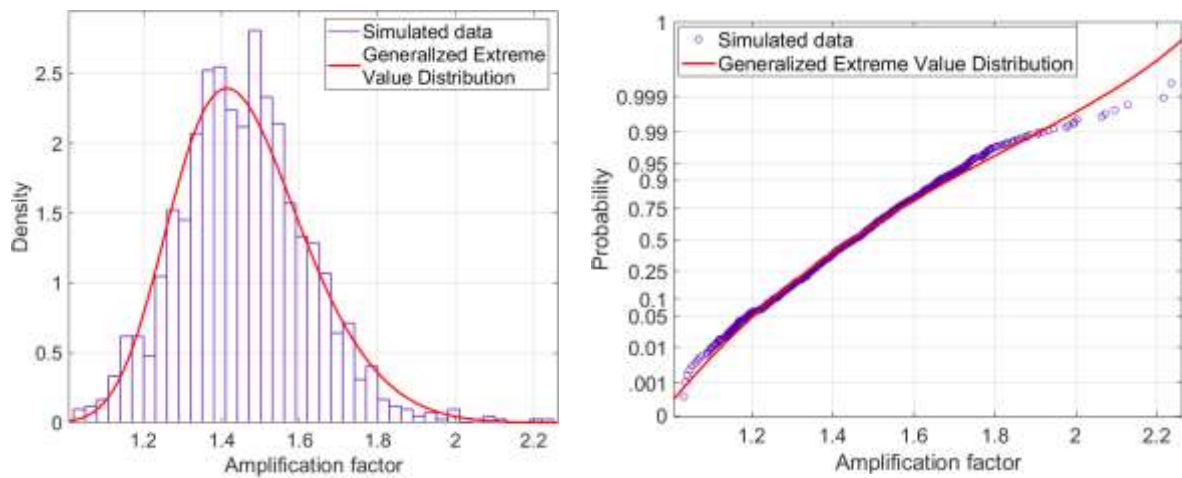


637 **Fig. 11.** Probability density function (left) and cumulative probability density function (right) derived using best  
 638 fit of gamma distribution for a sample of base curve values corresponding to a pacing rate 2.25 Hz and SDOF  
 639 natural frequency 24.8 Hz.

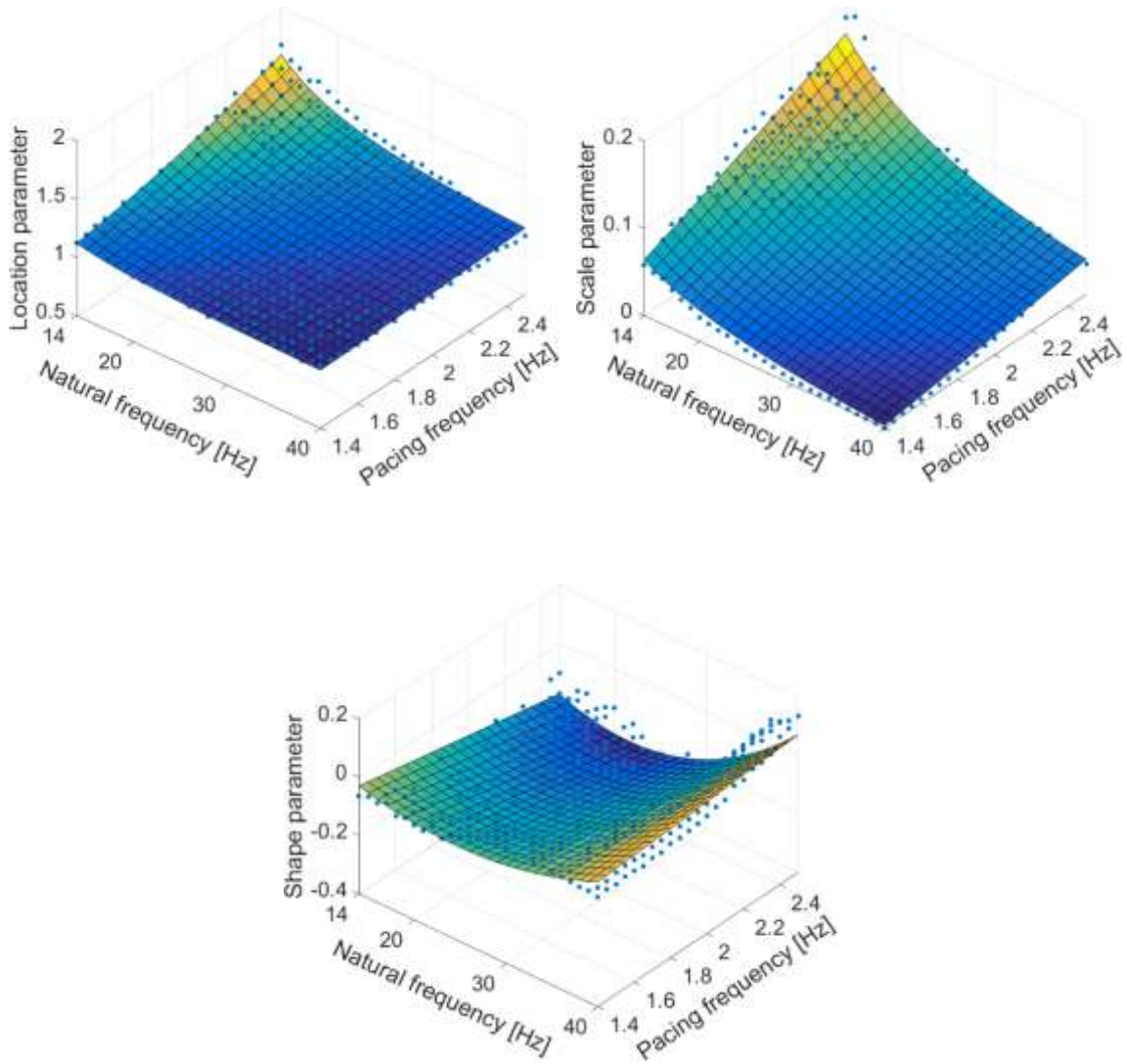


640 **Fig. 12.** Best fits of the shape (left) and scale (right) parameters for the gamma distribution.

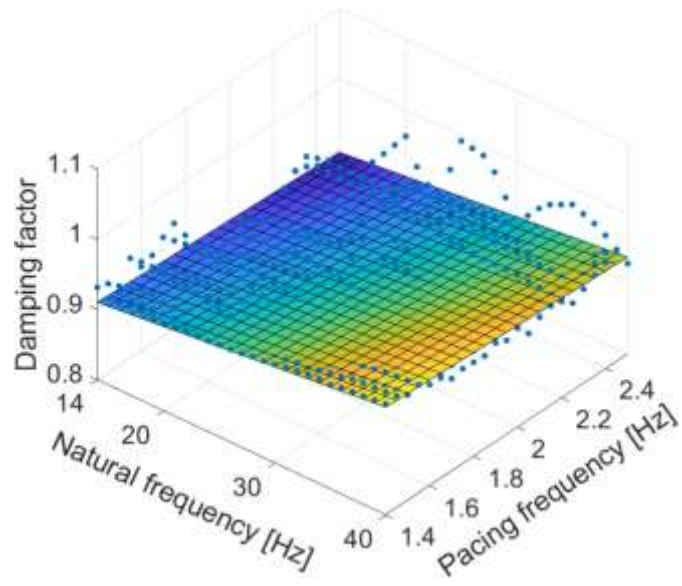
641



642 **Fig. 13.** Probability density (left) and cumulative probability density (right) functions using best fit of generalised  
 643 extreme value distribution for a sample of amplification factor values corresponding to a pacing rate of 2.25 Hz  
 644 and natural frequency of 24.8 Hz.



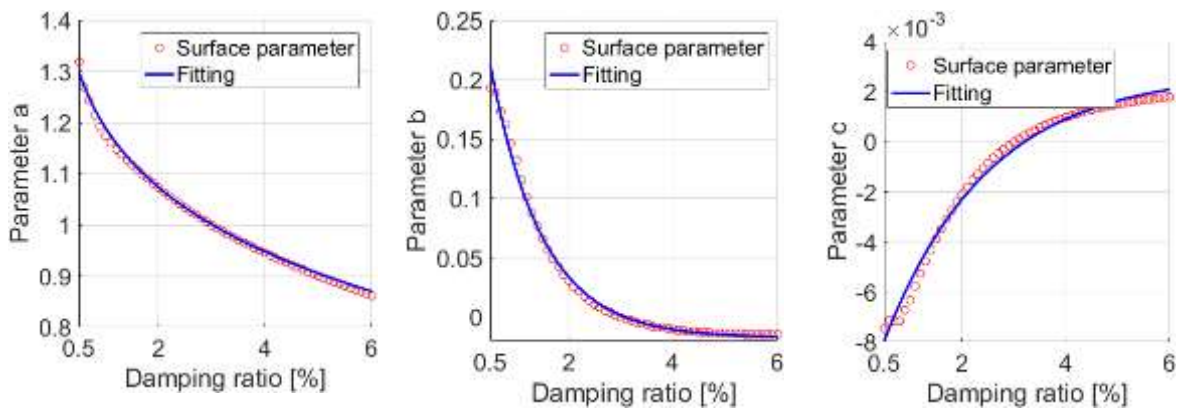
645 **Fig. 14.** Best fits of the location (top left), scale (top right) and shape (bottom) parameters for the generalised  
 646 extreme value distribution.



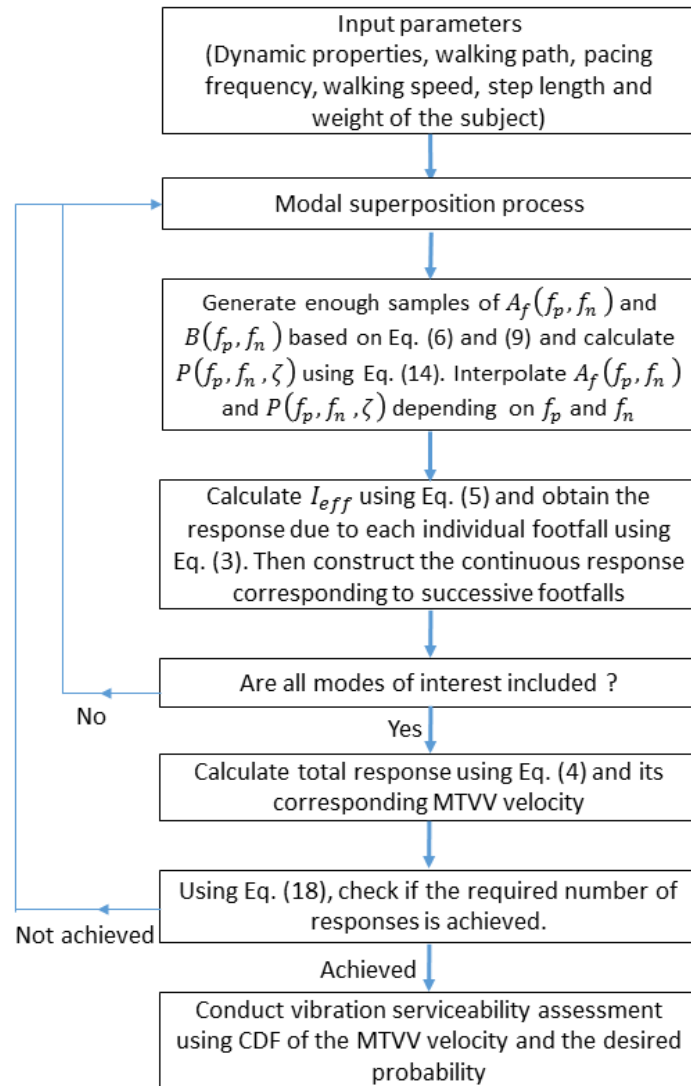
647

648 **Fig. 15.** Best fit of the damping factors corresponding to a damping ratio of 5%.

649



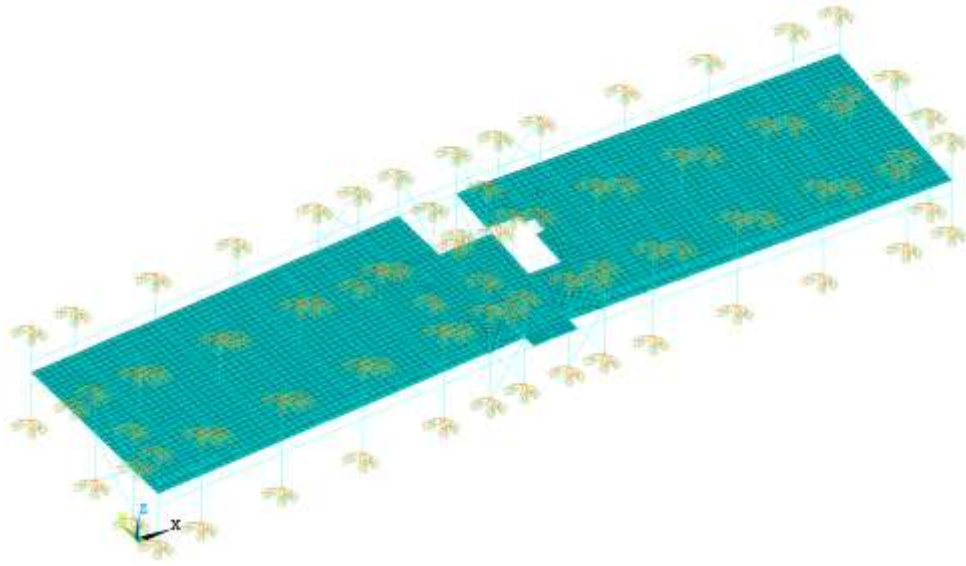
650 **Fig. 16.** Fitting parameters  $a$  (left),  $b$  (middle) and  $c$  (right).



651

652 **Fig. 17.** Implementation procedure of the new model.

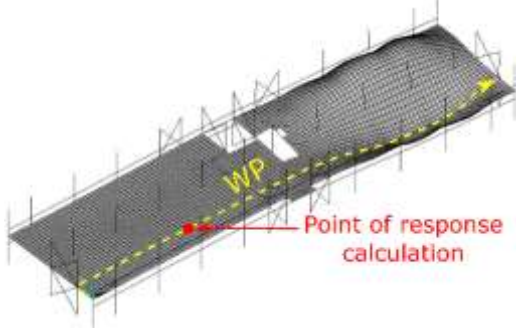




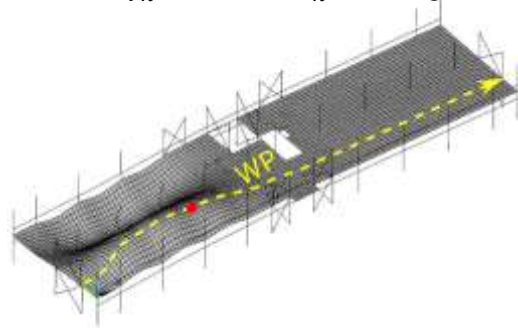
653

654 **Fig. 18.** FEM of the floor structure.

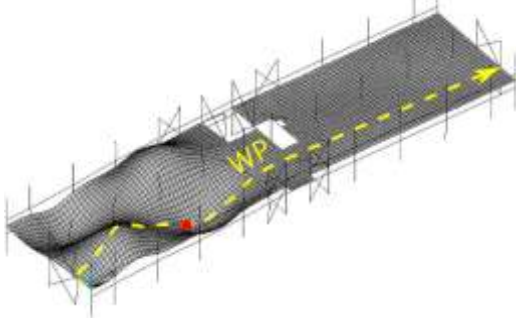
1<sup>st</sup> mode ,  $f_n=14.90$  Hz ,  $M_n=21780$  kg



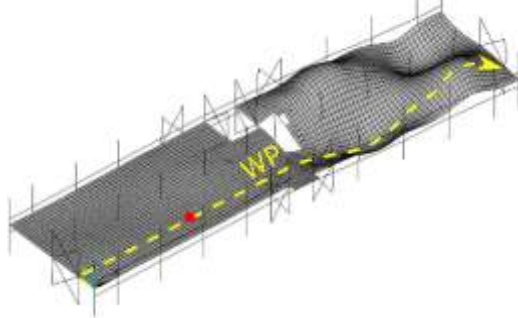
2<sup>nd</sup> mode ,  $f_n=14.91$  Hz ,  $M_n=22915$  kg



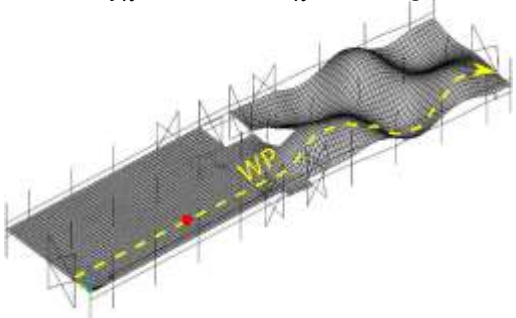
3<sup>rd</sup> mode ,  $f_n=15.32$  Hz ,  $M_n=21262$  kg



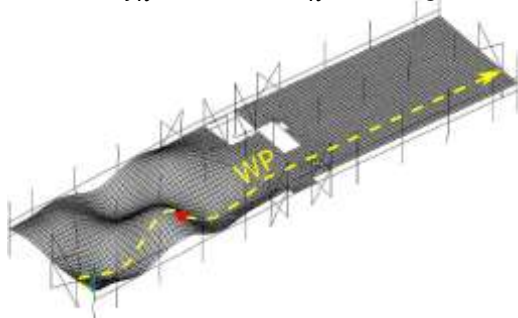
4<sup>th</sup> mode ,  $f_n=15.34$  Hz ,  $M_n=24338$  kg



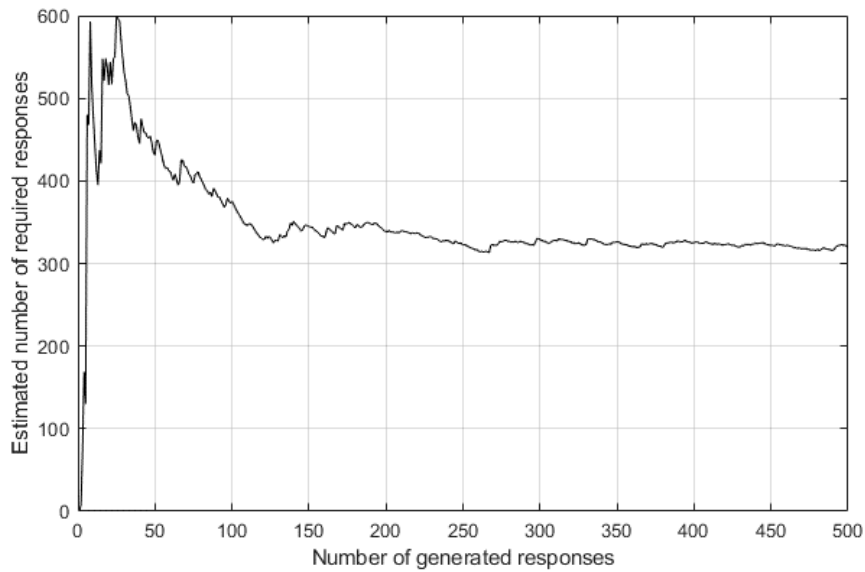
5<sup>th</sup> mode ,  $f_n=16.07$  Hz ,  $M_n=21237$  kg



6<sup>th</sup> mode ,  $f_n=16.16$  Hz ,  $M_n=14436$  kg



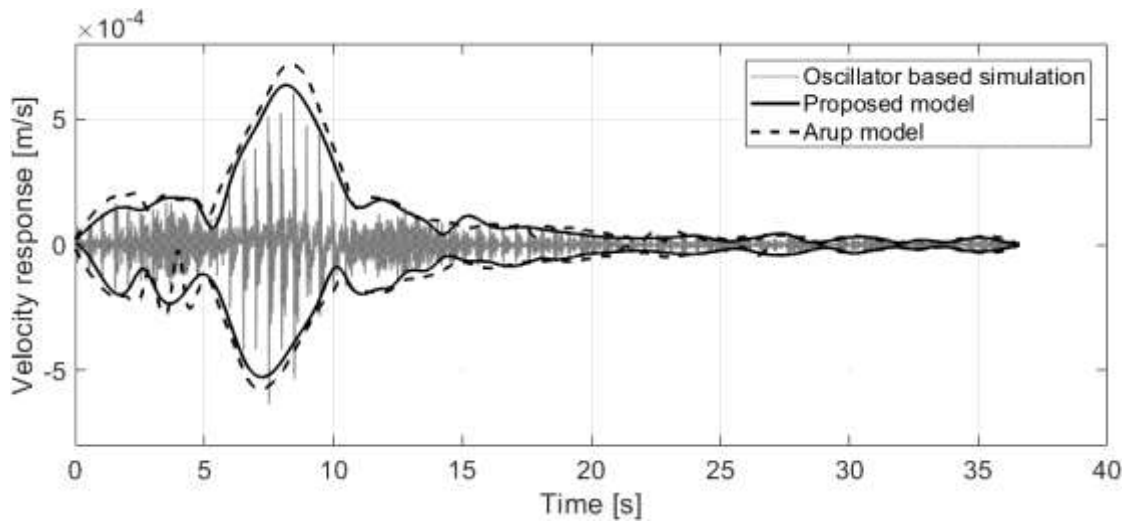
655 **Fig. 19.** Mode shapes, natural frequencies ( $f_n$ ) and modal masses ( $M_n$ ) of the first six modes showing the  
656 walking path (WP) (dashed yellow line) and the point of the response calculations (red dot).



657

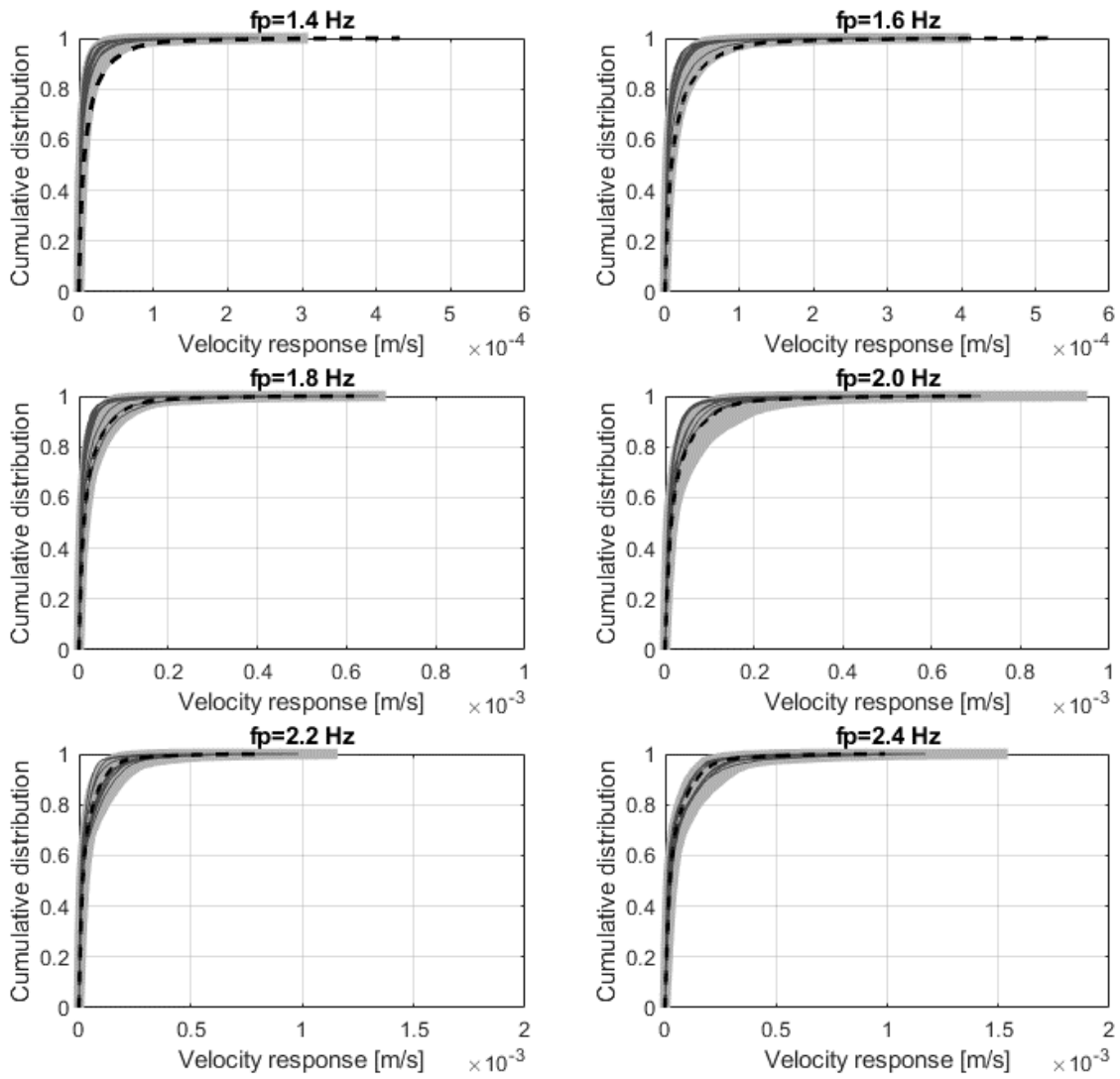
658 **Fig. 20.** Stability of the estimated number of the required simulations related to the response calculation at pacing  
 659 rate of 1.4 Hz. The required number of generated responses was achieved after 326 iterations.

660



661

662 **Fig. 21.** Time-history response samples from the oscillator based simulations, the new model and Arup's model  
 663 corresponding to a pacing rate of 2.0 Hz. For the responses calculated using the new model and Arup's model,  
 664 only their envelopes are shown in this figure for comparison purposes.



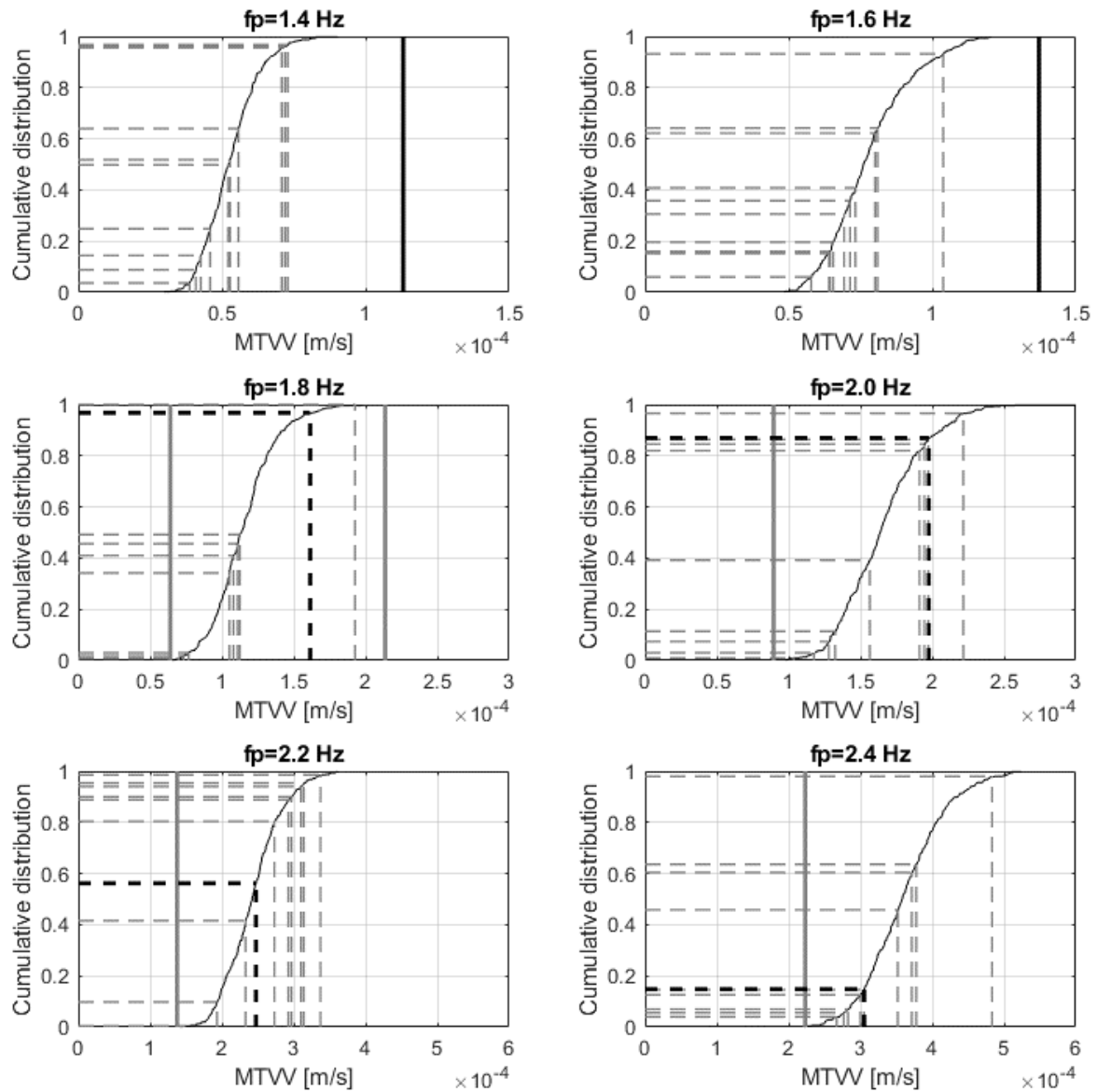
665

666

**Fig. 22.** Cumulative probability distribution function of the time history responses obtained from the new model

667

(light grey curves), oscillator based simulations (dark grey curves) and Arup's model (dashed black curves).



668

669 **Fig. 23.** MTVV velocity of the time history responses obtained from the new model (black thin curves), Arup's

670 model (black thick lines) and the oscillator based simulations (grey lines). Solid vertical lines represent the

671 values outside the ranges of the new model.

672 **Tables**

673 **Table 1.** Cut-off frequency between low- and high-frequency floors adopted by different authors and design  
 674 guidelines.

Author	Cut-off frequency
Ohlsson [36]	8 Hz
Wyatt and Dier [9]	7 Hz
Allen and Murray [37]	9 Hz
The Concrete Society [27]	10 Hz
The Concrete Centre [38]	10 Hz
The Steel Construction Institute P354 [39]	10 Hz for general floors, open plan offices etc 8 Hz for enclosed spaces, e.g. operating theatre, residential.
American Institute of Steel Construction [26]	9 Hz

675